UNIVERSITY OF CALIFORNIA,

IRVINE

Role of IRX5 in epidermal and hair follicle stem cells

DISSERTATION

submitted in partial satisfaction of the requirements

for the degree of

DOCTOR OF PHILOSOPHY

in Cellular & Molecular Biosciences

by

Jefferson K. Chen

Dissertation Committee:
Professor Bogi Andersen, M.D., Chair
Professor Xing Dai, Ph.D.
Professor Maksim Plikus, Ph.D.
Professor Anand Ganesan, M.D., Ph.D.

2021

Table of Contents

List of Figures

Acknowledgements

First and foremost I wish to thank my advisor, Dr. Andersen for his mentorship as this project would not have been possible without his guidance and patience. In addition, I am grateful to the members of the Andersen Lab who have helped me along my graduate career: Shuman, Bob, Julie, Junyan, Ghaidaa, Rachel, and Elyse.

This thesis would also have not been possible without the support of my students; Ly, Jude, Mahum, Clara, Jen, Sid, Evana, and Andre, who have provided tremendous assistance in my graduate work and have taught me how to be a better mentor.

I am grateful to my family who traded a comfortable life in a familiar country for a foreign land in the hopes that their children would have better opportunities. Their struggles as an immigrant family trying to find a way to make a living continues to inspire me to strive to work as hard as they did. In particular, I would like to thank: my grandparents, who raised me during the majority of my early youth and taught me how to be a more compassionate person. My dad, who trained as an architect in his home country yet commuted two hours every day to deliver mail so that I could have a better education. My mom and aunt, who pushed me to do the best that I can while also nurturing when I fell short. My partner, Miles, who has supported me at every step of my graduate career. This thesis would not have been possible without their unconditional support.

I'm deeply indebted to Dr. Tydell, Dr. Appleman, and Dr. Dennison, whose enthusiasm in teaching and science led me towards a career in research and medicine. My undergraduate research mentors, Dr. Qiao, Dr. Hunter, Dr. Varmus, Dr. Ponce, and Dr. Bardeesy, who have fostered an nurturing scientific environment and taught me how to become a better scientist.

Finally, I would like to thank the UCI SOM Biochemistry department and MSTP program for all the support over the many years. I would also like to acknowledge the National Institute of Child Health and Human Development for their support in funding this work through the F30 Ruth L. Kirschstein National Research Service Award.

Curriculum Vitae

Jefferson K. Chen

EDUCATION

University California, Irvine School of Medicine **2014 – Present**
Medical Scientist Training Program (MD/PhD)
PhD Candidate in Biochemistry

University California, Davis **2008 – 2012**
B.S., Environmental Toxicology

PUBLICATIONS

Chen JK, Wildermen J, Nguyen L, Lin J, Hui CC, Plikus M, Andersen B. Irx5 activates hair follicle stem cells through repression of cyclin kinase inhibitor p21. (In Progress)

Chen JK, Kashgari G, Andersen B. Capturing New Disease Genes in Psoriasis and Other Skin Diseases. Journal of Investigative Dermatology. 2021 Aug 1;141(8):1881–4.

Lin Z, Jin S, **Chen JK**, et al. Interfollicular epidermal differentiation is gradualistic rather than stepwise with GRHL3 controlling progression from stem to transition cell states. Nature Communications (2020)

Klein RH, Stephens DN, Ho H, **Chen JK**, Salmans ML, Wang W, Yu Z, Andersen B. Cofactors of LIM Domains Associate with Estrogen Receptor alpha to Regulate the Expression of Noncoding RNA H19 and Corneal Epithelial Progenitor Cell Function. J Biol Chem. 2016 Apr 29;jbc.M115.709386

Qiao H, **Chen JK**, Reynolds A, Hoog C, Paddy M, Hunter N. Interplay between Synaptonemal Complex, Homologous Recombination, and Centromeres during Mammalian Meiosis PLoS Genet. (2012) Jun;8(6):e1002790.

Reynolds A, Qiao H, Yang Y, **Chen JK**, Biswas K, Holloway K, Baudat F, Massy B, Wang J, Hoog C, Cohen P, Hunter N. RNF212 is a dosage-sensitive regulator of crossing-over during mammalian meiosis. Nature Genetics (2013) Mar;45(3):269-78.

AWARDS

NICHD F30 Ruth L. Kirschstein National Research Service Award MD/PhD Fellowship
2012 American Society for Microbiology Raymond Sarber Award Undergraduate Laureate
2011-2012 American Association for Cancer Research Bardos Science Education Award

RESEARCH EXPERIENCE

Biochemistry Graduate Student **11/2015 – Present**
Bogi Andersen, M.D., University of California, Irvine
Studied the role of Irx5 in epidermal differentiation and hair follicle stem cell activation

National Institutes of Health IRTA Fellow **9/2012 – 7/2014**
Harold Varmus M.D., National Cancer Institute
Investigated Nkx2-1 as a potential driver mutation in lung adenocarcinoma

Harvard Stem Cell Institute Summer Scholar **6/2010 – 9/2010**
Nabeel Bardeesy Ph.D, Massachusetts General Hospital
Examined the cellular plasticity of pancreatic ductal and centroacinar cells with KRAS mutation and P53 inactivation to characterize epigenetic drivers of pancreatic ductal adenocarcinomas

HHMI Summer Scholar, Undergraduate Research Associate **1/2010 – 6/2012**
Neil Hunter Ph.D, University of California, Davis
Characterized the role of SUMOlyzation protein, RNF212, in the post-translational modification of meiotic recombination proteins involved in homolog synapsis and recombination

Emergency Medicine Research Associate **9/2008 – 1/2011**
Abhi Gorhe M.B.B.S., University of California, Davis Medical Center
Assisted in data collection for ongoing clinical studies in the Emergency Department

Undergraduate Research Associate **2/2009 – 1/2010**
Reen Wu Ph.D, University of California, Davis
Characterized the signal transduction pathways of IL-17 mediated gene expression in human airway epithelia

California Institute of Technology Amgen Scholar **6/2009 – 9/2009**
Adrian Ponce Ph.D, NASA Jet Propulsion Laboratory
Validated and automated a novel bacterial endospore detector for water treatment and homeland security biodefense programs

Undergraduate Research Associate **6/2008 – 9/2008**
Maria Appleman Ph.D University of Southern California Keck School of Medicine
Assisted the development of a clinical study on effects of gastric bypass surgery on the gut microbiome

RELATED PROFESSIONAL EXPERIENCE

UC Irvine Counseling Center **3/2019 – Present**
LGBTQ Peer Mentor
Fostered an accepting environment to support students experiencing unique challenges associated with LGBTQ identity

UC Irvine DECADE PLUS **4/2016 – 6/2018**
Graduate Student Mentor
DECADE PLUS is a pilot US Department of Education college retention program for high achieving students from underserved communities. We developed curriculum to help students build academic skills while also conducting individual bi-weekly meetings with 5 assigned undergraduates.

National Science Bowl **4/2016 – Present**
Life Sciences Consultant
Wrote and reviewed biology questions to be used in the regional and national competitions

Journal of Young Investigators
Board of Directors **1/2019 – Present**
Serve in an advisory capacity to undergraduate volunteers

Chief Executive Officer **6/2013 – 9/2015**
Secured funding, oversaw major changes in internal staffing to improve project output and staff retention

Science and Career Center Director **6/2012 – 8/2013**
Created and maintained a large public database of all national research internships for students

Training Research Editor **8/2011 – 1/2013**
Revised and ran a 13-week training program which trained 40 incoming volunteer associate editors in peer review and data analysis to ensure robust scientific peer review

Biology Associate Editor **5/2010 – 8/2011**
Evaluated manuscript submissions bimonthly with faculty advisor

Whitman-Walker Health **11/2013 – 8/2014**
Peer Counselor Volunteer
Listened and provided objective support for LGBT youth facing issues ranging from family difficulties to HIV diagnosis

Abstract of the Dissertation

Role of IRX5 in epidermal and hair follicle stem cells

by

Jefferson K. Chen

Doctor of Philosophy in Cellular & Molecular Biosciences

University of California, Irvine, 2021

Professor Bogi Andersen, Chair

In tissues undergoing constant cellular turnover, DNA damage repair is critical as proliferating cells are prone to replication errors. Genomic instability, especially in adult stem cells, can result in senescence, apoptosis, or uncontrolled growth. Here, we focus on two stem cell types, hair follicle stem cells and basal keratinocytes, both of which rapidly proliferate to maintain tissue homeostasis. We characterize an novel transcription factor, IRX5, as a critical mediator of DNA damage repair and stem cell activation. In a *Irx5* knockout mouse model, HFSC exhibit prolonged senescence in part due to defective DNA damage repair. Furthermore, we identify FGF18 and BRCA1/BARD1 as downstream targets of IRX5.

Chapter 1. Background

Skin

The skin serves as a complex organ containing a diverse set of features that are critical for survival. The outer most layer, the epithelium, contains layers of keratinocytes that undergo biochemical and morphological changes to maintain a outermost layer of dead cornified cells that serves as protection from the external environment. This epidermal layer houses numerous specialized cells such as: Merkel cells, mechanoreceptors that relay light touch of the tissue to the CNS; Melanocytes which produce melanin, pigmented granules that are transferred to surrounding cells for UV protection; Langerhans cells, epidermal resident macrophages that responds to invading microbes and serve as antigen presenting cells. Below the epidermis, specialized structures such as hair follicles, sebaceous glands, and blood vessels act in synchrony to maintain tissue homeostasis such as thermoregulation and toxin secretion.

Epidermal differentiation

Epidermal differentiation occurs in three major instances: 1) In the initial development of the epidermis in late embryogenesis when surface ectoderm progenitor cells proliferate to give rise to differentiated progeny that form a stratified epithelium through progressive addition of cell layers (1); 2) During normal epidermal homeostasis in the adult when the epidermis rests in a homeostasis of balanced cell proliferation in the basal cell layer and cell death in the cornified layer (1,2); 3) In epidermal injury repair (3).

The epidermis is a stratified squamous epithelium containing a proliferating basal cell layer that gives rise to the suprabasally located post-mitotic keratinocytes. These keratinocytes undergo progressive specialization as they approach the surface where they terminally differentiate to form the stratum corneum, a layer of dead cells with crosslinked cornified envelopes (4). Numerous genes are activated in differentiating keratinocytes to form an effective permeability barrier. These genes primarily fall into four classes: 1) structural proteins like keratins, other cornified envelope components, and enzymes that crosslink these proteins (5); 2) adhesion molecules like tight junction and desmosomal proteins (6,7); 3) lipid producing enzymes required for lipids in the stratum corneum (8); 4) innate immunity components which protect the epidermis from microorganisms (9). While strong advances have been made (10), we don't fully understand the transcriptional mechanisms driving epidermal barrier formation.

Hair Follicle

Hair follicles serve as vital appendages for thermoregulation, sensation, and UV protection (11). Like the skin, hair follicles undergo constant replenishment which requires the activation and maintenance of pluripotent stem cells (12). Hair follicles are first developed in utero concurrently with prenatal epidermal development. Unknown activators drive keratinocytes to proliferate and form the hair placode. NfKB and Wnt signaling promote these epidermal cells to continue to proliferate and eventually forms the hair germ (13). A variety of activating signals such as Shh/Smo/Gli2, Wnt10, Lef1, and fibroblast growth factors continue to induce proliferation of these germ cells (14).

After birth, the follicle undergoes continuous regeneration through cycles of growth (anagen), destruction (catagen), and quiescence (telogen) of the hair fiber with each cycle resulting in a new hair fiber to take the place of the old shredded fiber (11).

The mature hair follicle base rests upon dermal cells, with the outer root sheath containing the hair follicle stem cells. Hair follicle stem cells undergo periods of quiescence and activation to replenish a pool of transit amplifying cells. These transit amplifying cells form the matrix, a bulbous condensation of cells located at the base of the hair follicle (15). Upon activation at anagen, the matrix cells proliferate and differentiate to form the Inner Root Sheath and hair shaft (13).

Balance between activation and quiescence is vital for HFSC population homeostasis. When in Telogen, the HFSC remain in a dormant state due to BMP signaling from a variety of sources. Adipocytes secrete BMP2 in a temporal pattern that aligns with the anagen to telogen transition while the dermal papilla and bulge inner layer secretes BMP6 (16,17). High levels of BMP maintains quiescence through NFATc1 mediated repression of cyclin activity (18). Expression of potent CDK inhibitors like CDKN1a (p21) is upregulated, fixing the cell in a dormant state (19). As the levels of BMP drop, Wnt and FGF7/10 signaling prevail and induce HFSC activation (20,21). This carefully controlled choreograph of quiescence/activation signal expression is mediated by transcription factors.

Transcriptional Regulation

Strong advances have been made in distinguishing factors which drive epidermal differentiation or hair follicle activation. Developmental transcription is driven by enhancers, positive DNA regulatory sequences residing few kb to 1Mb from their target promoters (22,23). Enhancers contribute to activation of target genes, which can be upstream, downstream, or within the enhancer, by serving as binding sites for transcription factors, co-activators, and histone modulators (24). Through advances in genomics, investigators have developed methods to identify global enhancer regions with the histone modification marks H3K4me1 and H3K27Ac (marks active enhancers) (25). These methods typically identify 20,000 to 150,000 enhancers per cell type, though not all of these enhancers are functional in promoting cell identity (26). Recent studies have classified enhancers as either typical enhancer (TE), 1-2kb long regions, or super-enhancers (SE), 12.5kb or larger regions with unusually strong enrichment of transcription factor binding, co-activator binding, and H3K27ac marks (27). Unlike TEs, SEs are thought to be particularly important for the specification of distinct cell types by driving gene expression programs unique to each cell type (28,29). To drive cell identity, SEs tend to be bound by a combination of unique transcription factors characteristic for that cell type (30).

Iroquois like homeobox domain is an example of such transcriptional regulator. First discovered in Drosophila, Irx homologs function early in development to differentiate the dorsal head and mesothorax, but also remain active in later stages of development to subdivide these territories (31,32). Irx homologs in Xenopus control cell fate decision between neuronal and epidermal lineages during embryonic neural plate

development (33). Like the epidermis, the neural plate is ectodermally derived, later invaginating along the midline, forming neural folds that then fuse to create the neural tube (34). The mammalian Irx gene family comprises of six genes (Irx1 – Irx6) in paralog pairs of Irx1/Irx3, Irx2/Irx5 and Irx4/Irx6 attributed to an ancestral duplication event(35). In vertebrates, Irx plays a major role in myocardial development (36), bone formation (37), and neuronal development (38).

A limited number of studies have implicated IRX5 in the regulation of cell cycle, apoptosis and cell migration (39–41). In adult vascular smooth muscle cells, IRX5 promotes G1/S transition through regulation of P27, E2F1, and PCNA (42). In hepatocellular carcinoma, IRX5 was also found to promote proliferation and also suppress apoptosis through regulation of BCL-2 (40). Studies in tongue squamous cell carcinoma attributed NFKB signaling to IRX5 in tongue squamous cell carcinoma proliferation and cell migration (39).

Cell cycle and DNA damage checkpoints

The cell cycle is a highly regulated process that is consecutively subdivided into growth (G1), DNA Synthesis (S), Mitosis preparation (G2), and Mitosis (M) (43). There are various checkpoints within the cycle to ensure proper cell growth and prevent uncontrolled cell proliferation, specifically with three main checkpoints: G1-S, G2-M, and metaphase-anaphase. The transition between phases at these checkpoints is dependent on the interaction between cyclin-dependent kinases (Cdks) and cyclin.

Throughout the entire cycle, cyclins expression is upregulated at specific cell cycle stages whereas the Cdk concentrations remain relatively constant.

Activated cyclin-Cdk complexes catalyze the progression of the cell cycle through subsequent phosphorylation of cyclin-Cdk substrates (43,44). Specific subsets of cyclins and Cdks are recruited and activated: Cyclin E-Cdk2, Cyclin A-Cdk1/Cdk2, and Cyclin B-Cdk1 complexes allow for the advancement to S phase, completion of S phase, and initiation of M phase, respectively (45).

The advancement through the G1-S checkpoint is characterized by a highly conserved DNA replication process that is initiated by activation of Cdks and Dbf4-dependent kinases (DDKs), which ultimately lead to the formation of replisomes that catalyze DNA replication (46). At this checkpoint, the integrity of the DNA is assessed for double-stranded breaks (DBSs) before engaging in DNA replication, ensuring genomic stability. One of the main regulators for this process is p53-binding protein 1 (53BP1) where it promotes DBS repair, specifically with non-homologous end-joining (NHEJ) (47). Upon the detection of a DSB on chromatin, 53BP1 accumulates around the DSB site to prevent DNA end resection, the initial process of homologous recombination DSB repair (47). Thus, 53BP1 directs the DSB site towards NHEJ as the primary form of DSB repair in the G1 phase (48).

Chapter 2: IRX5 promotes basal keratinocyte proliferation and DNA damage repair

Impaired epidermal differentiation and the resulting barrier defects underlie many skin diseases, including Atopic Dermatitis and Ichthyosis. Atopic Dermatitis, affecting 18% of all children and often observed within the first 6 months of life (49), is linked to genetic changes in the Epidermal Differentiation Complex (EDC), a 1.6Mb locus of 30+ genes encoding proteins that participate in barrier formation (50). Prominently, mutations in filaggrin, a resident in the EDC, have been identified as a strong predisposing factor for Atopic Dermatitis (51). Lamellar ichthyosis, characterized by an increase in cell proliferation and a delay in cell shedding during the first 2 weeks of life, has been linked to multiple regions of the genome, suggesting that a diversity of genetic defects gives rise to the ichthyosis phenotype (52). In particular, loss of TGM1, an enzyme involved in the formation of the cornified envelope, has been found to be one cause of lamellar ichthyosis (53,54). A fuller understanding of how transcription factors regulate differentiation and barrier formation may ultimately lead to new treatment ideas for diseases of defective barrier formation.

Grainyhead-like 3 (*Grhl3*), an example of such a transcription factor, serves as a key regulator of epidermal terminal differentiation and barrier formation during embryogenesis. Germline *Grhl3* knockout (ko) mice are embryonically lethal due to defective barrier formation, and neural tube defects, spinal bifida and exencephaly (55). The impaired epidermal barrier phenotype in *Grhl3* knockout mice is due to defective

activation of key gene expression programs required for cell adhesion, lipid production, cornified envelope formation, and protein crosslinking (56,57). Intriguingly, by modulating a gene expression program distinct from differentiation, *Grhl3* can also promote migration of keratinocytes for epidermal wound repair(58,59). These results indicate that *Grhl3* is an essential gene with evolutionary conserved function in epidermal development, wound repair, and neuronal development.

Enhancers regulating *GRHL3* are enriched with IRX motifs

Recent work characterizing enhancers and GRHL3 chromatin binding (60,61) in differentiating human keratinocytes identified changes in enhancer regions upon knockdown of *GRHL3*. While over half of typical enhancers are insensitive to GRHL3 levels, approximately 3,000 and 4,000 typical enhancers were lost and gained, respectively, upon *GRHL3* knockdown (61). Approximately 25% of gained typical enhancers and 10% of lost enhancers upon *GRHL3* knockdown correspond to regions that are normally directly bound by GRHL3. In contrast, only about 5% of unaffected *GRHL3* knockdown typical enhancers are bound by GRHL3, suggesting that in some cases binding of GRHL3 directly stimulates or suppresses active typical enhancer formation.

Genes linked to the newly gained typical enhancers are enriched in functional categories like spinal cord neuron specification, lymphocyte differentiation, and foregut morphogenesis (Fig. 2.1A). Lost typical enhancers contained genes involved in regulation of MAP kinase signaling, cell adhesion, wound repair, and cholesterol

metabolism – all of which are ontology categories associated with epithelial tissue (Fig. 2.1B). Mouse phenotype ontology of the genomic regions associated with gained typical enhancer include abnormal bone structure, whorled hair, abnormal vertebral morphology, and keratinocyte proliferation (Fig. 2.1C). In contrast, mouse phenotype ontology associated with lost typical enhancers include abnormal hemopoiesis, skin inflammation, abnormal stratum corneum, and corneal scarring (Fig. 2.1D). Previous studies have attributed GRHL3 to some of the mouse phenotype ontology associated with lost typical enhancers such as wound healing (62), corneal development (59), and epithelial barrier formation (57). These results indicate that the absence of GRHL3 results in the formation of new, heterologous typical enhancers that deviate from keratinocyte cell identity.

While knockdown of *GRHL3* resulted in the loss of only 4 super-enhancers, 58 new super-enhancers emerged (61). All of the regions corresponding to these newly formed super-enhancers after *GRHL3* knockdown are normally bound by GRHL3, compared to approximately 40% of random regions of similar size, suggesting that binding of GRHL3 directly suppresses the formation of heterologous super-enhancers in differentiated keratinocytes. Furthermore, many of the super-enhancers formed upon *GRHL3* knockdown are linked to genes with roles in neuronal migration and axon guidance, including *UNC5A* and Netrin. These gained super-enhancers upon *GRHL3* knockdown are strikingly enriched for a motif matching IRX4 (Fig. 2.1E). This suggests that GRHL3 functions in part to maintain epidermal cell fate by suppressing the formation of neuronal super-enhancers that in neuronal cells might be activated by IRX. Intriguingly,

many of the mouse phenotype ontology found in gained typical enhancers have been previously linked to IRX such as bone mineralization (37), neural patterning (63), and adipocyte thermogenesis regulation (64) (Fig. 2.1C).

Analysis of the super-enhancer that contains the *GRHL3* gene (Fig. 2.1F) revealed enrichment of IRX binding motifs, suggesting that IRX may play a role in regulating the expression of GRHL3 (Fig. 2.1G). Furthermore, the gene bodies of *IRX2*, *IRX4*, and *IRX5* also lie within differentiating super-enhancers, suggesting that *IRX* genes may also be regulated by the same enhancer program that regulates *GRHL3* expression (Fig. 2.1H). GRHL3 ChIP-seq revealed that GRHL3 binds on the gene bodies of *IRX1-6* (see representative examples in Fig. 2.1H,I). This indicates that GRHL3 may possibly also regulate *IRX* gene expression. *GRHL3* knockdown in differentiating human keratinocytes results in a slight decreased of *IRX2* expression (Fig. 2.1J) while *IRX2* knockdown results in decreased expression of *GRHL3* (Fig. 2.1K). Together, this data suggests a complex regulatory role between *GRHL3* and *IRX* that ultimately promotes the expression of epidermal differentiation genes.

IRX Depletion in keratinocytes result in downregulation of *GRHL3*

To determine the role of IRX in epidermal differentiation, we conduced siRNA knockdown of *IRX2*, *IRX4*, and *IRX5*, the top 3 highest expressing IRX genes during epidermal keratinocyte differentiation (Fig 2.2A). *IRX* knockdown experiments were done in 6 different donor human epidermal keratinocytes. Replicates were pooled for RNA-seq and selective results were confirmed with individual qPCR validation. For

knockdown experiments in differentiating keratinocytes, we transfected 30nM of siRNA in proliferating keratinocytes, then differentiation was induced with Calcium 15 hours later, and cells were collected 48 hours later.

Upon knockdown of *IRX4* and *IRX5*, a compensatory upregulation of *IRX3* expression is observed, suggesting potential cross regulation between *IRX* family genes or the existence of a compensatory mechanism (Fig. 2.2A). Knockdown of *IRX5* resulted in a three and two fold decrease in the expression of differentiation markers Involucrin and Keratin 1 respectively (Fig. 2.2B). Knockdown of *IRX2*, *IRX4*, and *IRX5* significantly affected the expression of *GRHL3* in both proliferating and differentiating keratinocytes (Fig. 2.2C), indicating that these *IRXs* potentially acts upstream of *GRHL3*.

Keratinocyte proliferation and differentiation segregate into distinct gene clusters

To characterize global changes in gene expression, bulk RNA sequencing was conducted with pooled siIRX knockdown experiments and we identified 821 differentially expressed genes ($p<0.05$) which clustered into 9 unique expression patterns among proliferating control, differentiated control, and differentiated siIRX knockdowns (Fig. 2.3A-B). Cluster 1-2 expression remained relatively unchanged during NHEK differentiation and contained genes involved in proliferation and cell signaling. Cluster 3-5, which are enriched in cell cycle activation and hemidesmosome genes, is characteristically expressed in proliferating keratinocytes. Cluster 6-9 gene ontologies are comprised of categories associated with differentiating keratinocytes like epidermal development, keratinization, cell-cell adhesion, and cornification (Fig. 2.3A-B). These 3

distinct gene expression clusters models the transcriptome changes observed during keratinocyte differentiation and serves as a reference for us to classify how IRX knockdown affects keratinocyte biology.

Knockdown of *IRX* downregulates cell cycle progression genes in differentiating keratinocytes

siIRX2, siIRX4, and siIRX5 knockdown samples all shared characteristic downregulation of cluster 4 which is highly enriched in cell cycle checkpoint genes. Closer analysis of the genes that contribute to mitotic and DNA repair GO categories in cluster 4 revealed enrichment of genes involved in G0/Early G1, G1/S transition, G2/M transition, prometaphase, mitotic spindle checkpoint, and anaphase. This category contains pro-proliferation genes RBL1 (65), *CDC6* (66), *MYBL2* (67), *CDK1* (68), and *CCNA2* (69). Master regulators of cell cycle progression, Cyclin A, Cyclin B, *CDK1* are significantly downregulated upon *IRX2* knockdown (Fig. 2.3A-B). Cyclin A binds to CDK2 to initiate DNA replication in S phase while at G2/M phase, Cyclin A binds with CDK1 to activate and stabilize the Cyclin B/CDK1 complex. Cyclin B/CDK1 complex forms at the onset of S phase and high levels of this complex triggers Mitosis initiation (43). These significantly downregulated Cyclins in siIRX2 suggests that *IRX2* promotes cell cycle progression during the S, G2, and M phase. siIRX4 and siIRX5 downregulated genes include genes that promote the G1/S and G2/M transition (Fig. 2.3 A-B). Downregulated cell cycle genes included *WSB2*, a gene involved in replication stress response at the G2/M checkpoint (70), and *CDK6*, a cyclin kinase which binds with Cyclin D to promote G1/S progression (71) (Fig. 2.3A-B).

Knockdown of *IRX5* resulted in unique gene expression changes not observed in the normal course of keratinocyte proliferation or differentiation. Cluster 2 is downregulated upon *IRX5* knockdown and contains genes involving regulation of TP53 activity (*PRDM1*,*BLIMP1*, *PDPK1*, *NUAK1*) and Type 1 Hemidesmosome assembly (*LAMB3*, *LAMA3*, *LAMC2*) (Fig 2.3B). PRDM1 is involved in the regulation of P53 and depletion of PRDM1 induces cell cycle arrest (72). Cluster 6 is upregulated only in the siIRX5 sample and not expressed in normal proliferating or differentiating keratinocytes. Cluster 6 includes genes like *NOTCH3*, a transmembrane protein that upon overexpression, induces cell cycle arrest through activation of CDH1 (73). All of these changes indicate that knockdown of *IRX5* results in an increased senescent state.

Collectively, these striking gene expression changes we observed in all *IRX* knockdown suggests that absence of IRX results in a more senescent state. It is unclear what role cluster 4 proliferating genes have in differentiating keratinocytes as proliferating gene programs are normally expressed in basal keratinocytes. However, the occurrence of the same proliferation defect among knockdown of *IRX2*, *IRX4*, and *IRX5* strongly suggests that IRX promotes proliferation regardless of the cell state.

IRX knockdown disrupts normal differentiation

Cluster 7-9 contains genes that are normally upregulated during keratinocyte differentiation but is downregulated upon knockdown of *IRX2, IRX4, and IRX5*.

Cluster 7 contains genes involved in keratinization, such as *FLG, LCE, KRT8, SPRR4* and is downregulated mainly in siIRX2 and siIRX5. Cluster 8 contains cornification genes such as *TGM1, SPRR2D, KRT13,* and *KRT16* and is downregulated in siIRX2 and siIRX4. Cluster 9, which contains epidermis development genes such as *CDSN, SPRR2A, KRT4, KRT7, KRT15,*and *CALML5*, is downregulated in all *IRX* knockdowns. While siIRX4 and siIRX5 seem to have moderate downregulation in these differentiation gene programs, siIRX2 displayed striking downregulation in all differentiation clusters.

IRX2 and IRX5 maintains differentiating keratinocyte identity

Cluster 6 gene expression is downregulated in proliferating keratinocytes and not expressed in differentiating keratinocytes. However, cluster 6 gene expression is notably upregulated in siIRX5. Many of the cluster 6 genes are prevalent in ovarian or breast carcinogenesis: The top ontology group includes Mucin O-linked glycosylation such as *MUC15* and *MUC16*. MUC16 is membrane bound and expressed in areas like the conjunctival and uterine epithelium where it contributes towards a dense mucinous gel layer as a protective layer against pathogens and external debris (74). Deregulated expression of *MUC16* has been linked psoriasis, Sjogren's syndrome, and cancer (75,76). *MUC16* has been linked to Psoriasis susceptibility locus 6 and while its role in psoriasis has not been characterized, *MUC16* has been shown to be expressed in the histology of psoriatic skin, with staining localized to basal epidermis and stronger expression in suprabasal cells (75). In ovarian cancer, *MUC16* is overexpressed and serves as a clinical marker (77). *FGFBP1*, which has been shown to be upregulated in breast and colon cancers, is also in Cluster 6 and upregulated upon IRX5 knockdown

(78). In skin, *FGFBP1* has been found to be significantly upregulated in invasive squamous cell carcinoma and also in psoriatic lesions but not in normal skin (79).

Cluster 1 is downregulated upon knockdown of *IRX2* and contains genes involved in AKT signaling and migration such as *AKT3*, *CHUK*, *FOXO3*, and *RUNX2*. RUNX2, a transcription factor, plays a crucial regulatory role in epidermal and hair follicle cells: *Runx2* null mice display delayed follicle maturation, reduced epidermal thickness, and reduced proliferation (80). In the hair follicle and epidermis, activation of AKT signaling induces proliferation (81). Cluster 5 is uniquely upregulated in siIRX2 samples and includes GO categories such as negative regulation of cell proliferation and IL-17/IL-10 signaling. Contributory GO category genes include *PTGS2*, *CXCL1*, *CXCL5*. *PTGS2*/*COX*-2, a prostaglandin signaling mediator, plays a critical role in epidermis and hair growth cycle. Transgenic overexpression models of *Ptgs2* exhibit reduced hair follicle density and delayed hair follow morphogenesis and epithelial hyperplasia due to aberrant epidermal differentiation (82).

Combined, these *IRX* knockdown experiments in differentiating keratinocytes reveal changes in global transcriptome that affect proliferation, differentiation, and cell identity. To better understand the role of IRX in proliferation, we conducted similar siIRX knockdown on proliferating keratinocytes.

IRX2 and IRX4 depletion in proliferating keratinocytes results in defective cell cycle checkpoint

Bulk RNA sequencing was conducted with pooled siIRX knockdown experiments and we identified 776 differentially expressed genes ($p<0.05$) which clustered into 8 unique expression patterns among proliferating control and proliferating siIRX knockdowns (Fig. 2.4A-E). To quantify the impact each *IRX* knockdown has on cell cycle during proliferation (Fig. 2.4B) and differentiation (Fig. 2.4C), we used Seurat's (83) cell cycle scoring function. Seurat analyzes the gene expression of known cell cycle regulators and produces an quantifiable value that is used to predict the sample's cell cycle stage. Knockdown of *IRX2* and *IRX4* in proliferation keratinocytes and differentiating keratinocytes results in G1 phase gene expression. However, only knockdown of IRX5 during differentiation results in G1 phase gene expression. These results suggests that *IRX2* and *IRX4* is needed for cell cycle progression.

Cluster 1-3, which is expressed in normal proliferating keratinocytes, is comprised of genes involved in cell cycle checkpoint. These include genes involved in G1/S and G2/M transition such as *E2F2, MYBL2, ORC1, and MCM10*. K-means clustering identified siIRX2 and siIRX4 proliferating keratinocytes with downregulated cell cycle checkpoint in cluster 1 and 2 (Fig. 2.4D-E). This suggests that *IRX2* and *IRX4* is upstream of critical cyclin activating factors.

IRX maintains basal keratinocyte state

Cluster 7 genes, which are upregulated upon knockdown of *IRX2*, contains keratinization genes such as *SPRR4* and Late Cornified Envelope genes (Fig. 2.4D-E). Previous in vivo and in vitro studies on keratinocytes have found that *SPRR4* is

normally expressed at low or undetectable levels but upon UV damage, is upregulated and incorporated into the damaged keratinocyte's cornified cell envelope (84). In addition, we also detected upregulated expression of *LCE3E*, another component of cornified cell envelope that is upregulated upon UV damage (85). This upregulation of aberrant UV induced differentiation factors in siIRX2 proliferating keratinocytes could be a consequence of inefficient DNA damage repair.

Cluster 5-6 is strikingly upregulated in siIRX4, contains gene ontologies such as retina morphogenesis, MAPK cascade involved in immune cell migration, and calcium concentration regulation. Retina morphogenesis include *PROX1*, a neuronal transcription factor expressed by neuronal stem cells during hippocampus development where it promotes cell cycle exit and neuronal differentiation (86).

Cluster 8, which is upregulated in the siIRX5 treated proliferating keratinocytes, contains enrichment of GO categories such as hair follicle differentiation and cell-cell junction (Fig. 2.4D-E). Aberrant upregulation of hair follicle factors such as *RUNX3*, which promote hair follicle development (87), *DSG1*, which plays an key role in hair follicle anchorage (88), and *SPINK6* was observed in siIRX5 treated proliferating keratinocytes. These finding suggests that *IRX5* maintains keratinocyte cell identity.

Collectively, our siIRX knockdown in proliferating keratinocytes reveal IRX2 and IRX4 as pro-proliferative factors necessary for cell cycle progression. Furthermore, we also

identify IRX2, IRX4, and IRX5 as factors which preserves basal keratinocyte cell identity.

Irx5$^{-/-}$ epidermis is intact and without pathology

To follow up on these in vitro results, we analyzed an global *Irx5* knockout mouse. *Irx5*$^{-/-}$ mice are embryonically viable with an intact epidermal barrier. Histology of *Irx5*$^{-/-}$ and *Irx5*$^{+/+}$ epidermis reveal no apparent pathology (Fig. 2.5A-C). Immunofluorescent staining of P20 adult mice back skin revealed normal K14 basal and LOR terminally differentiated epithelial layer (Fig. 2.5D-I).

IRX5 promotes keratinocyte proliferation

To characterize the aberrant gene programs in *Irx5*$^{-/-}$ epidermis, we isolated 20 day old whole epidermis of *Irx5*$^{-/-}$ (n=2) and *Irx5*$^{+/+}$ (n=2) mice for bulk transcriptome. We identified 478 upregulated genes and 1,513 downregulated genes in *Irx5*$^{-/-}$ epidermis (Fig. 2.5J-K). Gene ontology of downregulated genes revealed significant enrichment in pro-proliferation categories such as RNA metabolism, translation, and cell cycle (Fig. 2.5J). Consistent with our NHEK in vitro studies, downregulated genes in the cell cycle related ontology categories include cell cycle checkpoint and P53 dependent DNA damage response genes.

Upregulated genes in the *Irx5*$^{-/-}$ epidermis were enriched with ontology categories such as negative regulation of epithelial differentiation, hair follicle development, positive regulation of cell death, and negative regulation of cell proliferation (Fig. 2.5K).

Keratinocyte differentiation ontology included genes such as *Gata3, Hoxa7, Mycl, Numb, Xdh, Yap1, Spry2, Sgpp1,* and *Cd109*. Upregulated gene were also enriched with gene ontology category hair follicle development which include *Tgm3*. Previous work characterizing TGM3 have found that it does not play a role in epithelial barrier formation but is essential for hair follicle development (89).

Irx5$^{-/-}$ basal keratinocytes are more quiescent

To confirm these transcriptome findings of defective proliferation, we quantified proliferation with EdU in 20 day old *Irx5*$^{-/-}$ (n=4) and *Irx5*$^{+/+}$ (n=4) mice (Fig. 2.6A-B). Positive EdU staining was present throughout the basal layer. *Irx5*$^{+/+}$ keratinocytes were 8% EdU positive while *Irx5*$^{-/-}$ keratinocytes were 2% EdU positive (Fig. 2.6C). This result confirm that *Irx5*$^{-/-}$ basal keratinocytes are more quiescent than wild type basal keratinocytes.

IRX5 is protective against DNA damage

Our human keratinocyte transcriptome data indicate that knockdown of *IRX* results in an inability to clear the G1/S checkpoint, where DNA integrity is verified. Detection of DNA damage or replication error stabilizes P53 which in turn activates P21 to induce quiescence (90). γH2AX, an histone which binds to unrepaired DNA double stranded breaks (DSB), is rarely detected in the epidermis under physiological conditions (91). We did not detected any γH2AX staining in *Irx5*$^{+/+}$ epidermis (n=2) but found a small percentage of γH2AX positive keratinocytes in *Irx5*$^{-/-}$ epidermis (n=3) (Fig. 2.6D).

Presence of increased γH2AX staining in *Irx5*$^{-/-}$ keratinocytes suggests an impaired ability to repair DNA damage incurred from physiological conditions.

Upon DSB detection, γH2AX recruits factors such as P53, which then either mediates DNA damage repair, cell cycle arrest, or apoptosis. To determine if DNA damage in *Irx5*$^{-/-}$ keratinocytes is repaired, we conducted immunofluorescent staining of P53BP1, a DNA repair recruiting factor that promotes nonhomologous end joining mediated repair of DSB (92). Consistent with γH2AX staining, P53BP1 was rarely found in *Irx5*$^{+/+}$ epidermis but present in *Irx5*$^{-/-}$ keratinocytes in the form of sharp distinct focuses (Fig. 2.6G-I). Sharp distinct 53BP1 nuclear bodies is indicative of active DNA repair, suggesting that these *Irx5*$^{-/-}$ basal keratinocytes are undergoing replication stress and is stalled at G1/S (93).

Unrepaired DNA damage activates P21 cell cycle arrest in *Irx5*$^{-/-}$ keratinocytes

DNA damage activates P53-P21 induced cell cycle arrest, which allows the cell to repair the lesion before replicating (94). To determine if *Irx5*$^{-/-}$ basal keratinocytes are indeed experiencing stalled cell cycle, we quantified the prevalence of P21 (CDKN1A) in the epidermis (Fig. 2.6J-K). 8% of *Irx5*$^{+/+}$ keratinocytes were P21 positive compared to the 35% of keratinocytes in *Irx5*$^{-/-}$ epidermis (Fig. 2.6J-L). This 4 fold increase in P21 positive keratinocytes suggests that *Irx5*$^{-/-}$ basal keratinocytes are quiescent due in part to an activated DNA damage-P53-P21 pathway.

Discussion

We have characterized a novel transcription factor that plays an critical role in keratinocyte DNA damage repair. In proliferating and differentiating keratinocytes, IRX maintains keratinocyte identity. Absence of IRX2, IRX5, and IRX4 during differentiation results in aberrant keratinocyte differentiation, as observed by the upregulation of genes such as Mucin production and hair follicle development. In both proliferating and differentiating keratinocytes, we observed cell cycle defects upon knockout or knockdown of *IRX2*, *IRX4*, and *IRX5*. Upon knockdown of *IRX2* and *IRX4*, proliferating keratinocytes were stuck in the G1 phase, with specific downregulation of spindle assembly and DNA damage repair genes.

These in vitro findings was validated with an *Irx5*$^{-/-}$ mouse model. While the *Irx5*$^{-/-}$ mice epithelial barrier was intact, bulk transcriptome analysis reveal aberrant downregulation of proliferation genes. In basal keratinocytes, *Irx5* ablation results in accumulation of DNA DSB, which in turn induces P53-P21 mediated quiescence.

How IRX5 plays a role in both differentiation and proliferation is an intriguing question that requires further investigation. Previous studies on DNA damage in keratinocytes may provide some context. In keratinocytes overburdened with genotoxic stress, P21 is activated to promote differentiation (95). Recent studies have proposed an novel keratinocyte differentiation pathway – whereby DNA damage induced mitotic arrest is triggered to promote differentiation (96).

Keratinocytes have an robust DNA damage repair program – with many redundant factors promoting DNA damage repair. We have identified IRX5 as an novel factor that plays a key role in the DNA damage repair of basal epithelial cells. IRX5 may be a prognostic marker in epithelial based diseases such as breast, lung or ovarian carcinomas. While the effects of *Irx5* ablation seems to be limited in the epidermis, IRX5 could play a central role during massive epithelial repair such as barrier insults or UV radiation damage.

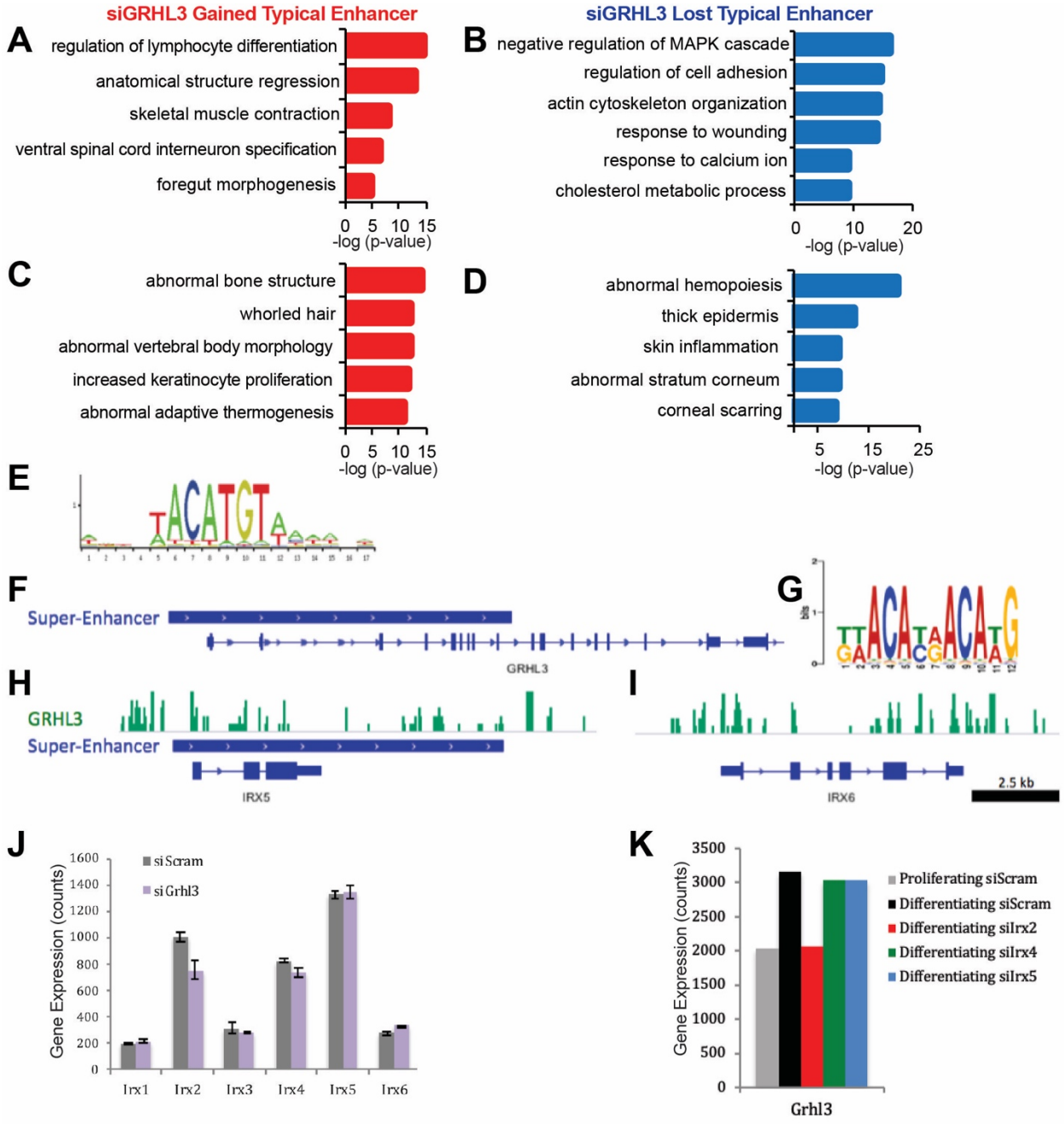

Figure 2.1: Unique epidermal enhancers in the absence of GRHL3

A) Gene ontology categories of TE gained upon GRHL3 KD. B) Gene ontology categories of TE lost upon GRHL3 KD C) Mouse phenotype ontology categories of TE gained upon GRHL3 KD. D) Mouse phenotype ontology categories of TE lost upon GRHL3 KD E) Irx4 motif enriched in SE gained after GRHL3 KD. F) Super-enhancer on the GRHL3 gene. G) Irx2 motif on the Grhl3 super-enhancer. (p=1e-16) H) The Irx5 gene is within a SE containing multiple GRHL3 peaks (in green). I) The IRX6 gene features GRHL3 binding but is not within a SE. J) Expression of Irx1-Irx6 in the knockdown of Grhl3. K) Expression of Grhl3 upon knockdown of Irx2, Irx4, and Irx5.

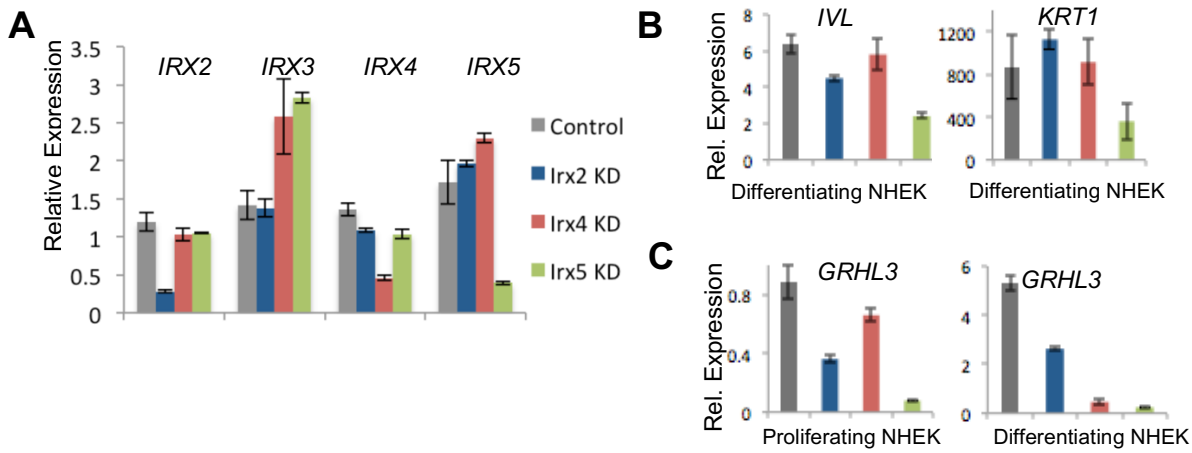

Figure 2.2: Gene expression changes after IRX knockdown
qPCR validation in differentiating siControl NHEK (n=6), differentiating siIRX2 (n=6), differentiating siIRX4 (n=6), and differentiating siIRX5 (n=6) for A) IRX gene expression, B) epidermal differentiation markers, and C) GRHL3 gene expression

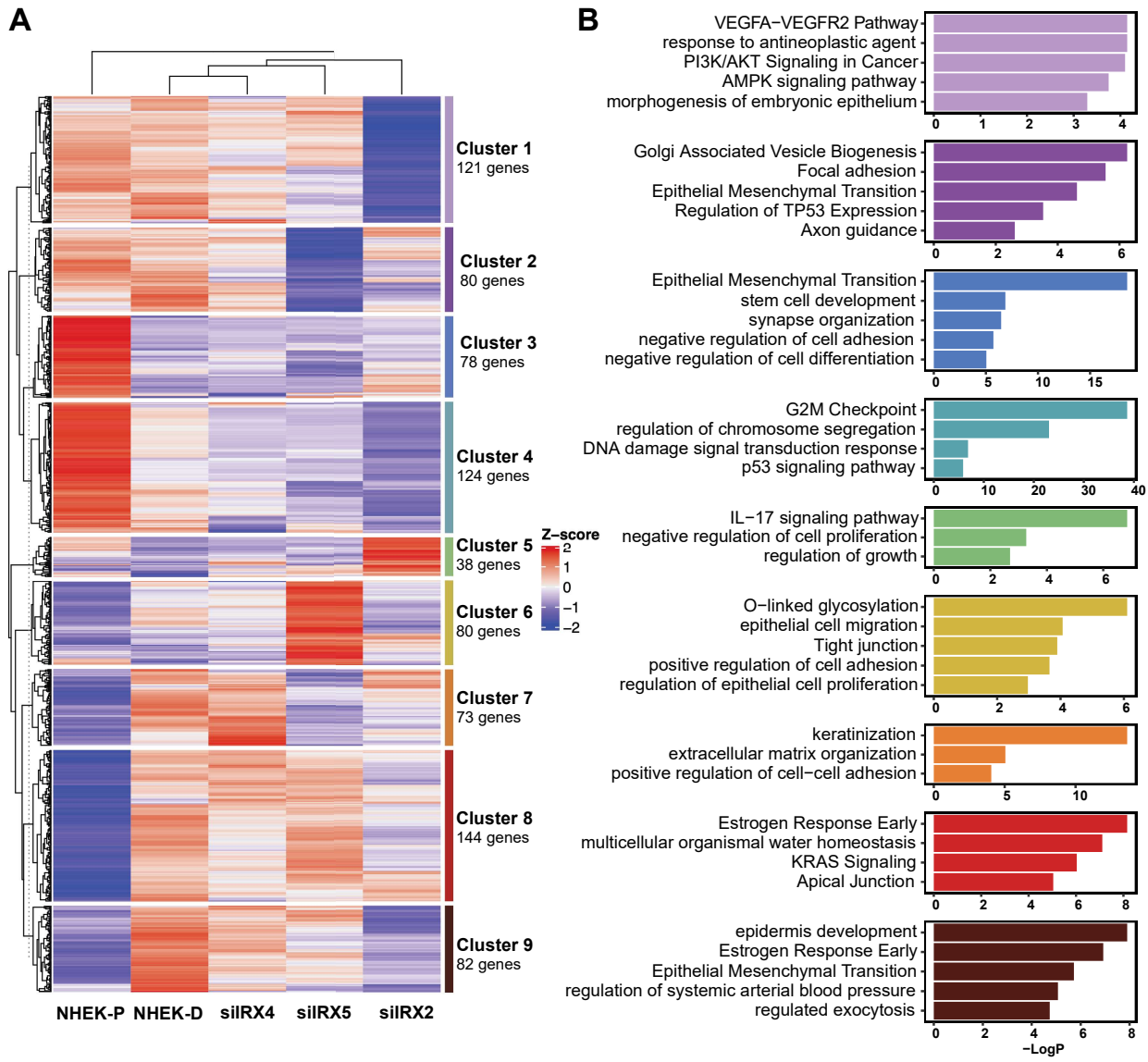

Figure 2.3: IRX in differentiating keratinocyte maintains keratinocyte cell state
A) NHEK-D IRX knockdown differential genes are clustered with K-means clustering. B) Gene ontology categories of each clusters.

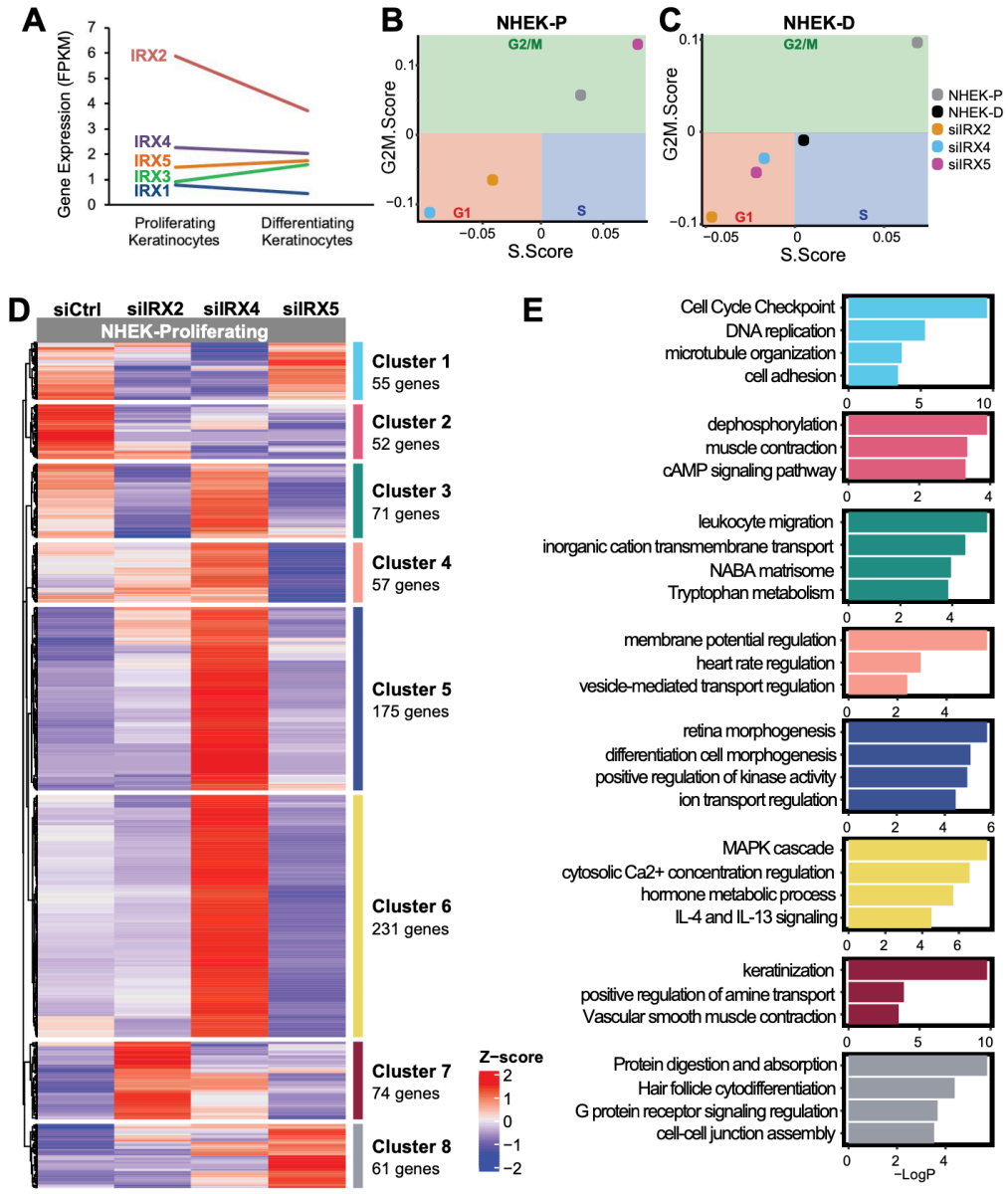

Figure 2.4: IRX factors promote human keratinocyte proliferation.
A) IRX1-5 gene expression in proliferating and differentiation keratinocytes. B-C) A Seurat scatter plot based on cell cycle score of controls and after siRNA knockdowns. After knockdowns of IRX factors, cell cycle gene expression becomes more characteristic with the G1 stage of the cell cycle. D) A heatmap showing hierarchical clustering based on transcript expression in control keratinocytes and after *IRX2*, *IRX4*, and *IRX5* siRNA knockdowns in NHEK-P. E) Top Gene Ontology categories of each cluster. Cluster 1 contains cell cycle and DNA damage related genes; these are downregulated upon knockdowns of *IRX2* and *IRX4*.

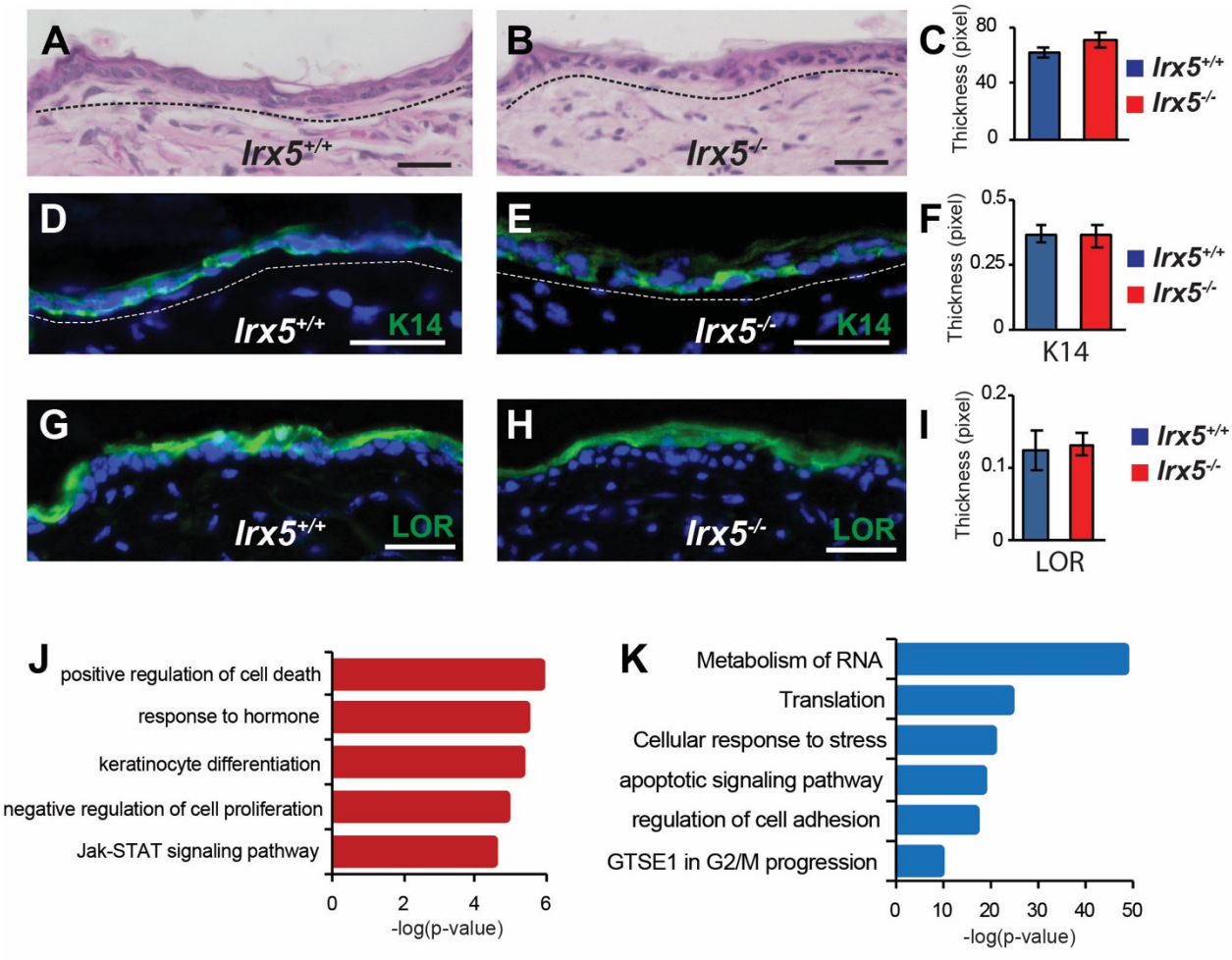

Figure 2.5: *Irx5*$^{-/-}$ epidermis is intact

A-B) Representative H&E images of 20 day old littermates. C) Measurement of epidermis thickness in *Irx5*$^{-/-}$ mice (n=2) and *Irx5*$^{+/+}$ mice (n=2). D-E) Representative images of K14 immunofluorescent staining in 20 day old littermates F) Quantification of K14, in *Irx5*$^{-/-}$ mice (n=2) and *Irx5*$^{+/+}$ mice (n=2) G-H) Representative images of LOR immunofluorescent staining in 20 day old littermates I) Quantification of LOR, in *Irx5*$^{-/-}$ mice (n=2) and *Irx5*$^{+/+}$ mice (n=2). J) Gene ontology of upregulated genes in P20 epidermis bulk RNAseq in *Irx5*$^{-/-}$ mice (n=2) and *Irx5*$^{+/+}$ mice (n=2). K) Gene ontology of downregulated genes in P20 epidermis bulk RNAseq in *Irx5*$^{-/-}$ mice (n=2) and *Irx5*$^{+/+}$ mice (n=2).

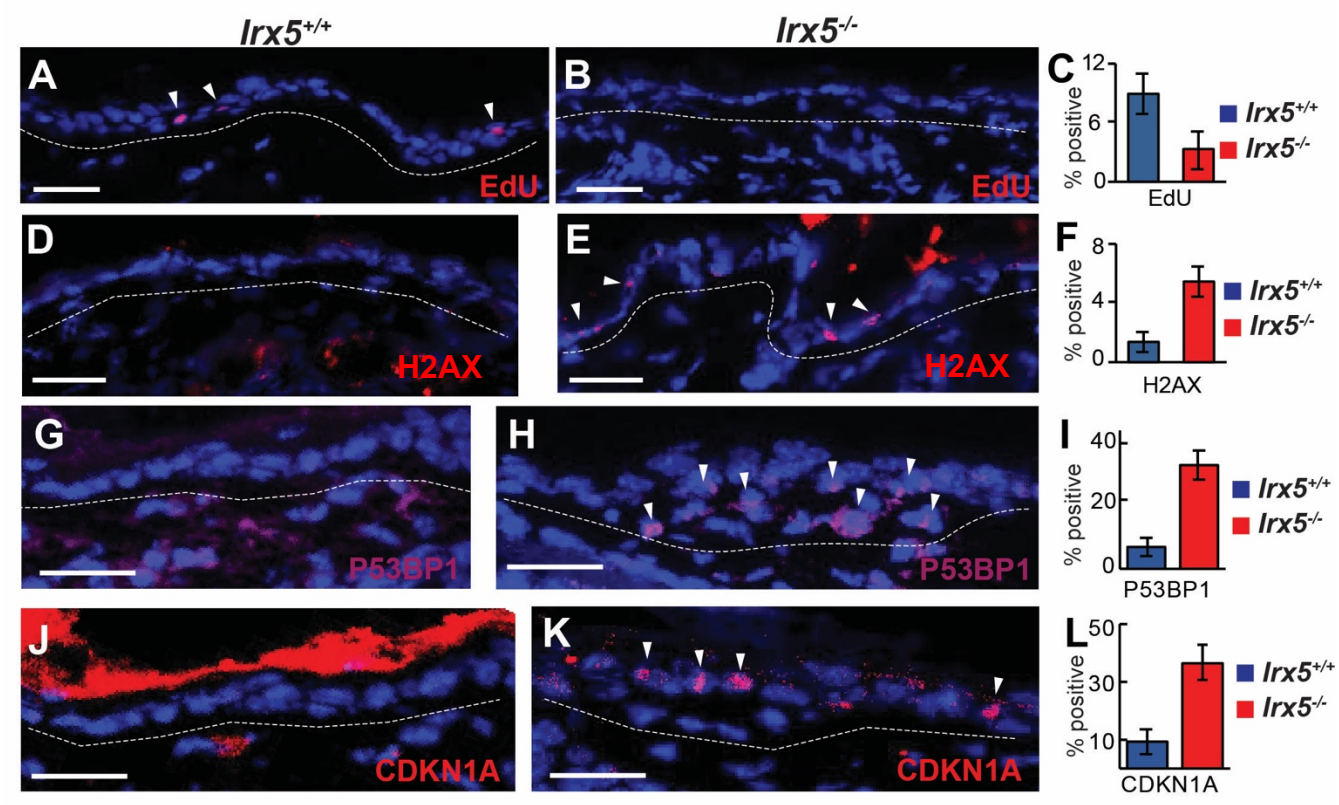

Figure 2.6: Activated P53-P21 DNA damage response in *Irx5*$^{-/-}$ epidermis

A-B) Representative images of EdU staining in 20 day old littermates. C) Quantification of % EdU positive cells in keratinocytes of *Irx5*$^{-/-}$ mice (n=4) and *Irx5*$^{+/+}$ mice (n=4). D-E) Representative images of H2AX immunofluorescent staining in 20 day old littermates. L) Quantification of % H2AX positive cells in keratinocytes of *Irx5*$^{-/-}$ mice (n=3) and *Irx5*$^{+/+}$ mice (n=2). G-H) Representative images of P53BP1 immunofluorescent staining in 20 day old littermates. I) Quantification of % P53BP1 positive cells in keratinocytes of *Irx5*$^{-/-}$ mice (n=2) and *Irx5*$^{+/+}$ mice (n=2). J-K) Representative images of CDKN1A immunofluorescent staining in 20 day old littermates. L) Quantification of % CDKN1A positive cells in keratinocytes of *Irx5*$^{-/-}$ mice (n=2) and *Irx5*$^{+/+}$ mice (n=2).

Chapter 3: IRX5 promotes hair follicle stem cell activation and DNA damage repair

Due to the cyclic nature of hair follicle growth, the hair follicle is an ideal organ to characterize the mechanisms that drive stem cell differentiation, identity, proliferation, and quiescence. Recent findings have identified a handful of transcription factors which regulate hair follicle stem cells (HFSC) cell states though different mechanisms. TCF3/4 represses HFSC activation when it forms a complex with TIE4 to represses HFSC but activates hair growth when bound to B-Catenin (97,98). In the telogen-anagen transition, NFATc1 prevents HFSC activation through repression of CDK6, a cyclin kinase that inactivates RB thus allowing G1/S progression (18,71). FOXC1 promotes quiescence through activation of *Nfatc1* and BMP signaling. In addition, FOXC1 promotes expression of intercellular adhesion molecules such as E-cadherin, which allows retention of the old bulge. (99,100). LHX2 promotes HFSC maintenance and also plays an essential role in hair follicle morphogenesis (101). Conversely, HFSC proliferation is driven by transcription factors like *Runx1*, which is expressed during anagen to inhibit P21 (19).

In tissues undergoing constant cellular turnover, DNA damage repair is critical as proliferating cells are prone to replication errors. DNA repair is also crucial for quiescent cells like HFSC, which reside in their niche over an extended period of time thus accumulating mutations from environmental insults (102). Adult stem cells have diverse methods for addressing DNA damage: In response to radiation, cycling intestinal stem

cells undergo apoptosis via LGR5 activated WNT signaling while quiescent intestinal stem cells are radioresistant in part due to SOX9 mediated repression of WNT signaling (103,104). In mammary stem cells, induced double stranded breaks (DSB) are efficiently repaired by p21 mediated Non-homologous end joining (NHEJ) (105,106). Melanocyte stem cells exposed to ionizing radiation triggers premature differentiation into mature melanocytes (107). Collectively, these findings indicate that cellular response to DNA damage is cell type dependent.

As one of the most prolific cycling stem cells, HFSC are at highly susceptible for acquiring DNA damage. Yet HFSC are radioresistant and readily repair DNA damage (108). While upper hair follicle cells and matrix cells respond to DNA damage with apoptosis, HFSC rely on elevated expression of DNA damage repair factors such as *Bcl-2* (108). BCL-2 suppresses DNA damage induced apoptosis and homologous recombination (HR), promoting the efficient but error prone NHEJ for DNA damage repair (109). In its quiescent phase, HFSC are resistant to DNA damage induced apoptosis in part due to anti-apoptotic factors like BCL-2 and stabilization of P53 (109,110). In the quiescent phase, HFSC induced with irreversible DNA damage undergo massive proliferation, driven by PI3K-Akt (111). If unresolved, acute accumulation of DSB results p53/p38 induced apoptosis (111). Aging HFSC accumulate DNA damage and is removed from the bulge through DNA damage induced terminal epidermal differentiation by COL17A1 proteolysis (112).

Very little is known about the transcriptional and epigenetic regulators that confers HFSC DNA damage resistance. BRCA1, a tumor suppressor with roles in DNA repair, DSB resection, chromatin remodeling, and cell cycle checkpoint is one such factor that is required for HFSC development and DNA damage repair (113–115). Here, we identify a novel transcription factor, IRX5, as another regulator which promote hair follicle activation and DNA damage repair in HFSC. With previously published FACS isolation of HFSC (CD34+, ITGA6+, SCA1-) (116), we were able to collect HFSC from the back skin of normal and *Irx5*$^{-/-}$ mice at mid-telogen (P18) and late telogen (P20) (Fig. 3.1). RNA sequencing and ATAC-seq of these samples provided us with a global perspective of the cellular changes that occur in the absence of IRX5.

Irx5 is expressed in proliferating hair follicle stem cells

In public datasets of P5 isolated hair follicle cells (117), *Irx5* is expressed in hair follicle stem cells as well as in matrix cells (Fig. 3.2A). In comparison to key HFSC regulators, *Irx5* expression is at similar levels to *Jund* and *Foxc1*. Furthermore, *Irx5* expression follows a similar spatiotemporal pattern across the hair follicle differentiation trajectory, with *Irx5* expression highest in HFSC. Together, this suggests that *Irx5* is expressed in HFSC at levels similar to that of known HFSC regulators.

IRX5 binding motifs are enriched in hair follicle stem cell super-enhancers

HFSC drives hair growth through its distinct multi-step differentiation, requiring changes in its epigenetic landscape (118). These epigenetic alterations shift transcriptional circuitries which then direct lineage commitment. To determine if IRX5 is involved in

HFSC transcriptional circuitries, we analyzed previously published HFSC super-enhancers (119) as well as HFSC open chromatin for IRX5 motif enrichment (120). In open chromatin unique to HFSC, IRX5 motifs were enriched to a level comparable to that of the top five HFSC transcriptional regulators (Fig. 3.2B). Examination of HFSC super-enhancers also revealed that IRX5 motifs were enriched to levels higher than NFATc1, RFX2, and NFIB motifs (Fig. 3.2C). Collectively, these findings suggest that like known HFSC transcription factors SOX9 and NFATc1, IRX5 regulates critical HFSC genes.

Irx5 expression in the bulge increases from telogen to anagen

Fluorescent in situ hybridization (RNA-FISH) shows that *Irx5* mRNA is expressed in the bulge and secondary hair germ at P20 (late telogen) (Fig. 3.3A). Its expression increases by P28 and P32 (anagen) (Fig. 3.3B), when it is found at high levels within matrix cells with an asymmetric distribution (Fig 3.3A). Following up on this analysis, we isolated HFSC during mid-telogen (p18) and late telogen (p20) for bulk transcriptomics.

In normal hair follicles at P18, *Irx5* and *Irx6* are highly expressed while *Irx1, Irx2, Irx3, and Irx4* expression is low (Fig. 3.3C). By P20, expression of *Irx1-5* increases while *Irx6* expression is downregulated. Of note, *Irx5* is the highest expressing *Irx* at P20. In comparison to cultured human keratinocytes, *IRX2* is the highest expressing *IRX* (Fig. 2.4A). Ablation of *Irx5* in mouse HFSC result in compensatory upregulation of *Irx1-4* at P18 and *Irx1-3* at P20 (Fig. 3.3C). Cross-regulation of *IRX* was observed in human knockdown experiments as well, with knockdown of *IRX5* upregulating *IRX3* by 2 fold

(Fig. 2.2A). The expression of Irx5 in proliferating cells of the late telogen and anagen hair follicles is consistent with a role in proliferation of HFSC and their progeny.

Irx5 promotes anagen initiation and proliferation of hair follicle progenitors

Entering first telogen, *Irx5*$^{-/-}$ mice displayed thinning of the hair coat. To understand the cause of the hair loss in *Irx5*$^{-/-}$ mice, *Irx5*$^{-/-}$ and *Irx5*$^{+/+}$ littermates were shaved at P20 to observe hair growth throughout first anagen (Fig. 3.4A-B). *Irx5*$^{+/+}$ mice displayed new fur growth at the dorsal anterior region at postnatal age 30 (P30) whereas *Irx5*$^{-/-}$ mice remained bare. By P34, hair growth was visible at all shaved regions in *Irx5*$^{+/+}$ mice while no visible fur growth was observed in *Irx5*$^{-/-}$ mice. *Irx5*$^{-/-}$ mice initiated hair growth at P37, seven days later than its *Irx5*$^{+/+}$ littermate controls. Furthermore, hair regeneration in the *Irx5*$^{-/-}$ mice initiated at the dorsal center region with regeneration moving laterally while *Irx5*$^{+/+}$ littermate control hair regeneration in the anterior-posterior direction. These data indicate that IRX5 promotes anagen initiation and suggest that it may have a role in the activation of HFSC and other hair progenitors.

Analysis of hair follicle histology confirmed the delay in anagen initiation in *Irx5*$^{+/+}$ mice (Fig. 3.4C). From morphogenesis (P1) to catagen (P16), *Irx5*$^{-/-}$ and *Irx5*$^{+/+}$ mice display similar histology. By anagen (P24), a clear delay in the transition between telogen to anagen is observed in *Irx5*$^{-/-}$ follicles. *Irx5*$^{+/+}$ follicles displayed an enlarged matrix while *Irx5*$^{-/-}$ follicles displayed late-telogen histology. At *Irx5*$^{+/+}$ mid-anagen (P26), *Irx5*$^{-/-}$ follicles displayed a thin epithelial column characteristic of anagen entry. By P32, *Irx5*$^{+/+}$ follicles displayed regression of the epithelial column, indicative of catagen. *Irx5*$^{-/-}$

displayed a dramatically thickened dermis containing the lower bulb, suggesting the follicle had reached mid-anagen. By P46, *Irx5*$^{+/+}$ follicles exhibited telogen morphology while *Irx5*$^{-/-}$ follicles reached late anagen. By P56, *Irx5*$^{-/-}$ follicles exhibited telogen morphology.

Analysis of Auchene, Awl, Guard, and Zigzag hair fibers found no difference in hair fiber length and percent composition of back fur (Fig. 3.4D-F).

To investigate the cause of delayed anagen in *Irx5*$^{-/-}$ hair follicles, we quantified proliferation with EdU at p20, p28 and p32 (Fig. 3.5A). At p20, EdU was observed mainly in the hair germ of *Irx5*$^{+/+}$ hair follicles, with less EdU staining observed in the bulge. In comparison, *Irx5*$^{-/-}$ hair germ and bulge rarely had EdU staining in the hair germ, with 1% of EdU positive cells in the lower bulge (Fig. 3.5B). By P28, *Irx5*$^{+/+}$ hair follicles displayed increasing proportion of EdU positive cells in the lower matrix. *Irx5*$^{-/-}$ hair germ and bulge remained at 1% of all cells displaying EdU signal (Fig. 3.5C). By mid-anagen (P32), proliferating cells were prominently stained in the lower matrix of *Irx5*$^{+/+}$ hair follicles and still displayed higher proportion of EdU positive cells than *Irx5*$^{-/-}$ bulge (Fig. 3.5D). These data indicate that Irx5 deficient bulge cells are quiescent with matrix cells displaying proliferation defects.

Cell cycle progression gene expression is downregulated in *Irx5*$^{-/-}$ Telogen HFSC

To characterize the pro-proliferative role of IRX5, we isolated *Irx5*$^{-/-}$ and *Irx5*$^{+/+}$ HFSC from two telogen time points, P18 (n=3 *Irx5*$^{-/-}$, n=2 *Irx5*$^{+/+}$) and P20 (n=4 *Irx5*$^{-/-}$, n=4 *Irx5*$^{+/+}$) (Fig. 3.6A).

Principle component analysis clustered P20 *Irx5*$^{+/+}$ HFSC at the distal end of PC1, followed by P18 *Irx5*$^{+/+}$ HFSC, P18 *Irx5*$^{-/-}$ HFSC, and P20 *Irx5*$^{-/-}$ HFSC at the opposite end. As the major difference between P18 and P20 *Irx5*$^{+/+}$ HFSC is quiescence gene signature, we suspected PC1 variance was derived from cell cycle stage. If accurate, this would suggest that the further the timepoint is from mid-telogen, the more divergent the gene expression changes between the genotypes would be. To characterize the cell cycle gene expression differences, we used Seurat's (83) cell cycle scoring function. Seurat analyzes the gene expression of known cell cycle regulators and produces an quantifiable value that is used to predict the sample's cell cycle stage. As expected, P20 *Irx5*$^{+/+}$ HFSC were predicted to be proliferating while P18 samples and P20 *Irx5*$^{-/-}$ HFSC were predicted to be quiescent (Fig 3.6B).

Differential gene analysis between P18 *Irx5*$^{-/-}$ and *Irx5*$^{+/+}$ identified 2,259 downregulated and 630 upregulated genes. Differential gene analysis between P20 *Irx5*$^{-/-}$ and *Irx5*$^{+/+}$ identified 1,668 downregulated and 1,464 upregulated genes. K-means clustering of these samples revealed distinct clusters (Fig. 3.6C), allowing us to isolate IRX5 regulated genes independent of HFSC follicle stage. Cluster 6 gene expression remained static between P18 and P20 *Irx5*$^{+/+}$ HFSC, suggesting that gene expression of

this cluster is independent of the hair cycle. In both P18 and P20, cluster 6 genes were upregulated in *Irx5*$^{-/-}$ HFSC, suggesting that these genes are repressed by IRX5 regardless of the hair cycle stage (Fig. 3.6D). Cluster 6 is enriched with genes involved in negative regulation of cell proliferation such as *Klf4*, a growth arrest factor that induces the expression of CDKN1A (121). Upon DNA damage, KLF4 binds to SP1 motifs present on *Cdkn1a* promoter which then recruits P53 to drive *Cdkn1a* transcription (122). This could suggest a potential pathway in which the pro-proliferation factor IRX5 suppresses expression of anti-proliferation regulators.

Cluster 4, which is enriched with cell cycle progression genes, was differentially downregulated in *Irx5*$^{-/-}$ HFSC at P20 (Fig. 3.6C-D). These genes were primarily involved in the G1/S transition which included *Ccne1*. CCNE1 accumulates during G1/S boundary and forms a complex with CDK2. This complex serves as a central regulator of the G1/S transition which in part does so through activation of P220, a critical cell cycle progression factor that promotes transcription of histone H2B (123). Inhibition of H2B function results in cell cycle arrest, defective chromosomal segregation, and attenuated DNA damage response (124,125). This suggests that IRX5 acts upstream of critical DNA damage response programs in part by upregulating the expression of *Ccne1*.

Cluster 3 is also of particular interest as its gene expression is downregulated in *Irx5*$^{-/-}$ HFSC in both P18 and P20 time points. Cluster 3 is enriched with gene ontology terms such as Histone H3.1 complex organization and positive regulation of cell cycle (Fig.

3.6D). Histone H3.1 complex organization genes include *Chaf1a*, *Asf1b,* and *Ipo4*. CHAF1A is a critical subunit of Histone H3.1, a transient histone that is required for DNA replication and DNA repair (126,127). Downregulation of these critical cell cycle progression histone subunits occur both at P18 and P20, raising the possibility that IRX5 is a direct regulator of histone subunits required for changes to the epigenetic landscape.

Collectively, these findings indicate that IRX5 plays an pro-proliferative role in HFSC through repressing key negative regulators of cell proliferation and/or promoting the expression of histone subunits necessary for cell cycle progression.

IRX5 promotes key DNA damage repair factors

Differential gene analysis of P20 *Irx5*$^{-/-}$ and *Irx5*$^{+/+}$ HFSC identified *Brca1* and *Fgf18* as one of the top genes that are downregulated and upregulated respectively in *Irx5*$^{-/-}$ HFSC (Fig. 3.7A). Downregulated genes in *Irx5*$^{-/-}$ HFSC are significantly enriched with cell cycle checkpoint and DNA repair (Fig. 3.7B) whereas upregulated genes in *Irx5*$^{-/-}$ HFSC are enriched with positive regulation of cell death (Fig. 3.7C). Many of the downregulated DNA damage repair proteins such as *Brca1*, *Bard1*, *Mlh1*, *Fancd2*, *Rad51,* and *Exo1* are critical for DNA damage repair (Fig. 3.7D). From P18 to P20, the expression of these critical DNA damage repair genes in *Irx5*$^{+/+}$ HFSC is dramatically upregulated, suggesting these DNA damage repair proteins are necessary throughout the duration of proliferation (Fig. 3.7D). Furthermore, these genes are downregulated in

Irx5$^{-/-}$ HFSC during both P18 and P20, suggesting that IRX5 may be a direct regulator of these critical DNA damage repair genes.

BRCA1, a well-studied tumor suppressor, is a key regulator in DNA damage induced cell cycle checkpoint activation, DNA damage repair, transcriptional regulation, and apoptosis (128,129). Intriguingly, *Brca1* deficient mice display reduced hair follicles with increased DNA damage, and activated p53 dependent apoptosis in HFSC (113). Furthermore, BRCA1, BARD1, and RAD51, all of which are downregulated in *Irx5*$^{-/-}$ HFSC, are indispensable for homologous recombination (130). These differential genes were then analyzed with Qiagen Ingenuity Pathway Analysis, which predicted an increase in DNA damage, activated ATM/MAPK pathway, stabilized TP51, activated CDKN1A, and inhibited cell proliferation in *Irx5*$^{-/-}$ HFSC (Fig. 3.7E).

To characterize the deficient DNA damage repair identified from our transcriptome analysis, we conducted *Brca1* RNA in-situ hybridization in *Irx5*$^{-/-}$ and *Irx5*$^{+/+}$ hair follicles at P20, P28, and P32. *Brca1* expression is present in the P20 hair germ of *Irx5*$^{+/+}$ hair follicles. By P28 and P32 *Brca1* expression markedly increases in *Irx5*$^{+/+}$ matrix, with the majority of the expression localized to the lower bulge. In comparison, *Irx5*$^{-/-}$ hair follicles expressed *Brca1* at to low levels at P20 and P28. By P32, *Brca1* expression was found in the lower bulge of *Irx5*$^{-/-}$ mice, though at lower concentrations than P32 *Irx5*$^{+/+}$ hair follicles (Fig. 3.8B). Taken together, this data suggests that *Irx5*$^{-/-}$ HFSC have diminished DNA damage repair capabilities, which may contribute to the proliferation defect.

IRX5 modifies the epigenetic landscape

From our P18 and P20 transcriptome dataset, we identified altered histone regulation in *Irx5*$^{-/-}$ HFSC and wondered if this influenced the epigenetic landscape of *Irx5*$^{-/-}$ HFSC. We conducted Assay for Transposase-Accessible Chromatin (ATAC) sequencing on FACS-isolated HFSC from the back skin of *Irx5*$^{-/-}$ (n=2) and *Irx5*$^{+/+}$ (n=2) mice at P20. We identified an averaged total of 20,970 peaks in *Irx5*$^{+/+}$ and 32,692 peaks in *Irx5*$^{-/-}$ HFSC. The majority of differentially open chromatin were unique to *Irx5*$^{-/-}$ HFSC; differential peak analysis identified 4,277 unique peaks in the *Irx5*$^{-/-}$ and 5 unique peaks in *Irx5*$^{+/+}$ HFSC (Fig. 3.9A). We next analyzed the open chromatin regions for ontology enrichment of known mouse phenotypes, using the Genomic Regions Enrichment of Annotations Tool (131). *Irx5*$^{+/+}$ HFSC open chromatin regions were enriched in ontology categories related to epidermal function (Fig. 3.9B). However, *Irx5*$^{-/-}$ differential open chromatin contained mouse phenotype ontology related to abnormal DNA repair and early cellular replicative senescence, demonstrating that the majority of the aberrant unique open chromatin in *Irx5*$^{-/-}$ HFSC regulate genomic regions involved in DNA repair (Fig. 3.9C).

We overlapped these differential open chromatin regions with P20 HFSC differentially expressed genes in Binding and Expression Target Analysis to infer potential mechanisms mediated by *Irx5* (Fig. 3.9D,F). The majority of *Irx5*$^{-/-}$ HFSC unique open chromatin reside near mitotic cell cycle process genes, which are downregulated in *Irx5*$^{-/-}$ HFSC (Fig. 3.9F). Furthermore, these *Irx5*$^{-/-}$ unique open chromatin are enriched with

NFY-a motifs (Fig. 3.9G), which have been found to have a repressive nature towards cell cycle progression genes (132). In sum, these results suggest that in the absence of IRX5, epigenetic modifications occur near pro-proliferation genes so that E2F and DREAM complex is recruited to repress cell cycle.

IRX5 prevents DNA damage induced quiescence

To confirm if IRX5 is involved in DNA damage repair, we conducted protein immunofluorescence staining on key DNA damage markers. H2AX, which marks unrepaired double stranded breaks (133), was significantly elevated in *Irx5*$^{-/-}$ hair germ with 10% of all hair germ cells displaying positive H2AX staining while only 2% of hair germ exhibited H2AX staining in *Irx5*$^{+/+}$ hair germ (Fig 3.10A-B). Surprisingly, quiescent bulge cells displayed DSB at significant levels – 4% of cells are H2AX positive in the *Irx5*$^{-/-}$ bulge (Fig. 3.10B). Quiescent HFSC is highly resistant to DNA damage as its high expression of Non-Homologous End Joining (NHEJ) DNA repair factors like BCL2 readily repair the damage (108). The unusual presence of H2AX foci in *Irx5*$^{-/-}$ bulge indicates that IRX5 plays a critical role in NHEJ DNA damage repair. Furthermore, 53BP1, a DNA damage early response protein that promotes NHEJ repair, was also present at significant levels in the *Irx5*$^{-/-}$ bulge (Fig. 3.10C-D). Together, these results indicate that *Irx5*$^{-/-}$ bulge accumulate DNA damage due to a diminished DNA damage repair program.

Accumulated DSB results in enhanced ATR- dependent signaling which pushes the cell to undergo P21-mediated cell cycle exit (134). In the *Irx5*$^{-/-}$ bulge, CDKN1A is markedly

elevated compared to its wild type counterpart (Fig 3.10E-F). These results suggests that defective DSB repair inhibited cell cycle progression in cells without IRX5; thus contributing to the delay in anagen initiation.

IRX5 represses FGF18-induced HFSC quiescence

Fgf18 was one of the highest differentially elevated gene detected in *Irx5*$^{-/-}$ HFSC. As a signaling molecule, *Fgf18* is a critical downstream target of *Foxp1* that maintains HFSC quiescence (135,136). In the hair cycle, *Fgf18* is expressed at high levels during telogen to maintain telogen and inhibit anagen initiation (137). Studies on the radioresistant properties of FGF18 have found that FGF18 inhibits irradiation induced apoptosis and promotes DNA damage repair by activating ATM induced cell cycle arrest (138). To characterize the expression of *Fgf18*, we conducted in situ hybridization on hair follicles at various stages of telogen (Fig. 3.11A-D) and anagen (Fig. 3.11F-G) During telogen, Fgf18 is highly expressed until early anagen, where its expression markedly drops (Fig. 3.11E). However, in *Irx5*$^{-/-}$ hair follicles, *Fgf18* continues to be expressed throughout anagen (Fig. 3.11G). When compared to its wild type counterpart, *Irx5*$^{-/-}$ hair follicles shows a significant upregulation of Fgf18 signal at anagen.

To determine the role Fgf18 has in the phenotype of *Irx5*$^{-/-}$ hair follicles, we conducted inhibitor trials. We used a pan-FGFR inhibitor, AZD4547, to rescue the *Irx5*$^{-/-}$ telogen delay. *Irx5*$^{-/-}$ mice were treated with 10uM/g AZD4547 (n=11) every two days from p20 to p46, *Irx5*$^{-/-}$ were treated with 1% DMSO saline (n=9), and *Irx5*$^{+/+}$ littermates were treated with 1% DMSO saline (n=7). With the pan-FGFR inhibitor, we observed a partial

rescue of 4 days, with 100% back fur recovery in AZD4547 treated *Irx5*$^{-/-}$ group compared to the untreated *Irx5*$^{-/-}$ group. From these results, we have identified a pathway controlled by IRX5 in cell cycle regulation.

Discussion

Adult stem cells which reside long term in their niche are at risk for accumulating DNA lesions. While some stem cells respond to DNA damage by inducing apoptosis or premature differentiation, HFSC are resistant to DNA damage due to their robust DNA damage repair (108). Here, we have identified IRX5 as an novel pro-proliferation factor that promotes DNA damage repair in HFSC as well as its progeny.

Irx5 deletion in mice results in delayed anagen as a consequence of defective proliferation and increased DNA damage. In the absence of IRX5, quiescent and proliferating cells are both more susceptible to DNA damage. During first telogen, we detected accumulated DSB in *Irx5*$^{-/-}$ quiescent HFSC which resulted in P53-P21 mediated senescence. Through epigenetic and transcriptomic analysis, we have characterized repressive SP1 and NFY-A enriched motifs near critical cell cycle progression genes that is present only in *Irx5*$^{-/-}$ HFSC. Furthermore, we identified IRX5 as a upstream regulator of critical DNA damage repair mediators BRCA1 and BARD1. We have also identified IRX5 as an upstream repressor of FGF18, which plays a key role in maintaining HFSC quiescence during telogen.

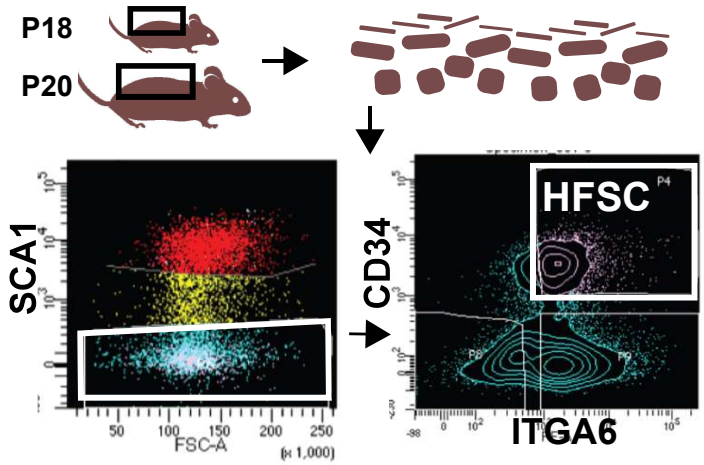

Figure 3.1: Hair follicle stem cell FACS isolation
P18 and P20 *Irx5*$^{+/+}$ and *Irx5*$^{-/-}$ mice back skin was processed into a single cell suspension and FACS sorted for Sca1- CD34+ ITGA6+ HFSC. RNA sequencing was conducted with the isolated cells.

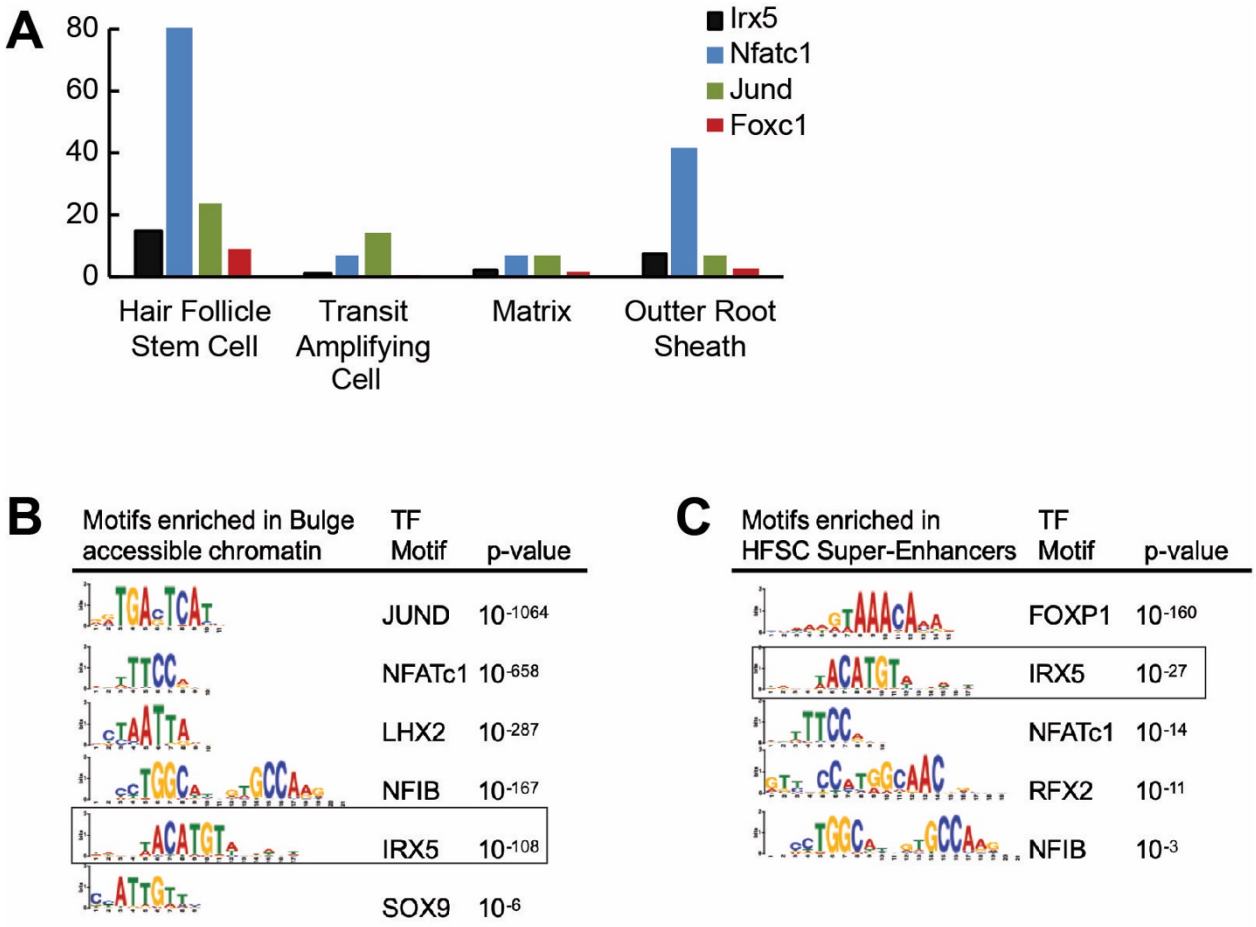

Figure 3.2: IRX5 is expressed in hair follicle stem cells

A) mRNA expression of key HFSC regulators in Rezza et al. published RNAseq dataset of P5 isolated mouse hair follicle cells. B) Enriched motifs identified from Adam et al. (2018) isolated bulge ATAC-seq. C) Enriched motifs identified from Adam et al. (2015) identified bulge super-enhancers.

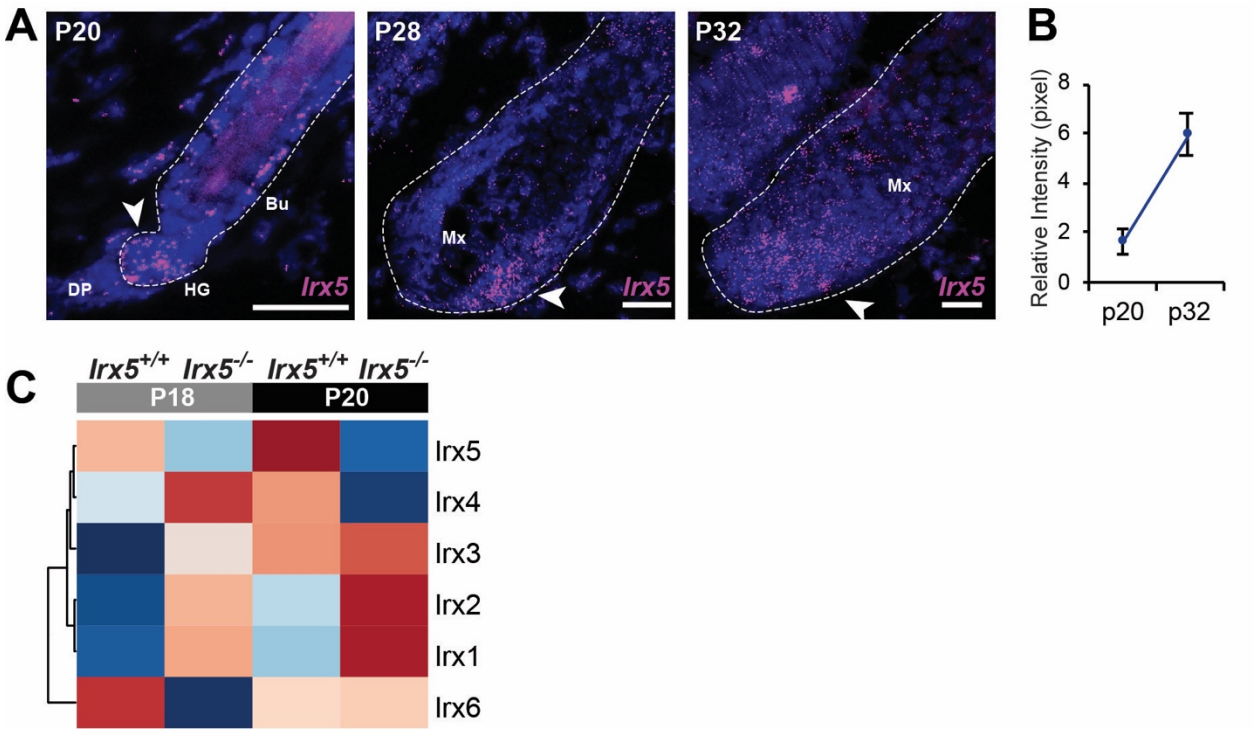

Figure 3.3: Irx5 is expressed during telogen and anagen

A) *Irx5* RNA fluorescent in-situ hybridization in normal mouse hair follicles from postnatal day (P) 20, 28 and 32. Arrows indicate areas of strong Irx5 expression. B) Quantification of Irx5 signal intensity in the hair follicle lower bulge at P20 (n=4) and at P32 (n=2). C) Expression of *Irx1*, *Irx2*, *Irx3*, *Irx4*, *Irx5*, and *Irx6* in sorted P18 and P20 HFSC.

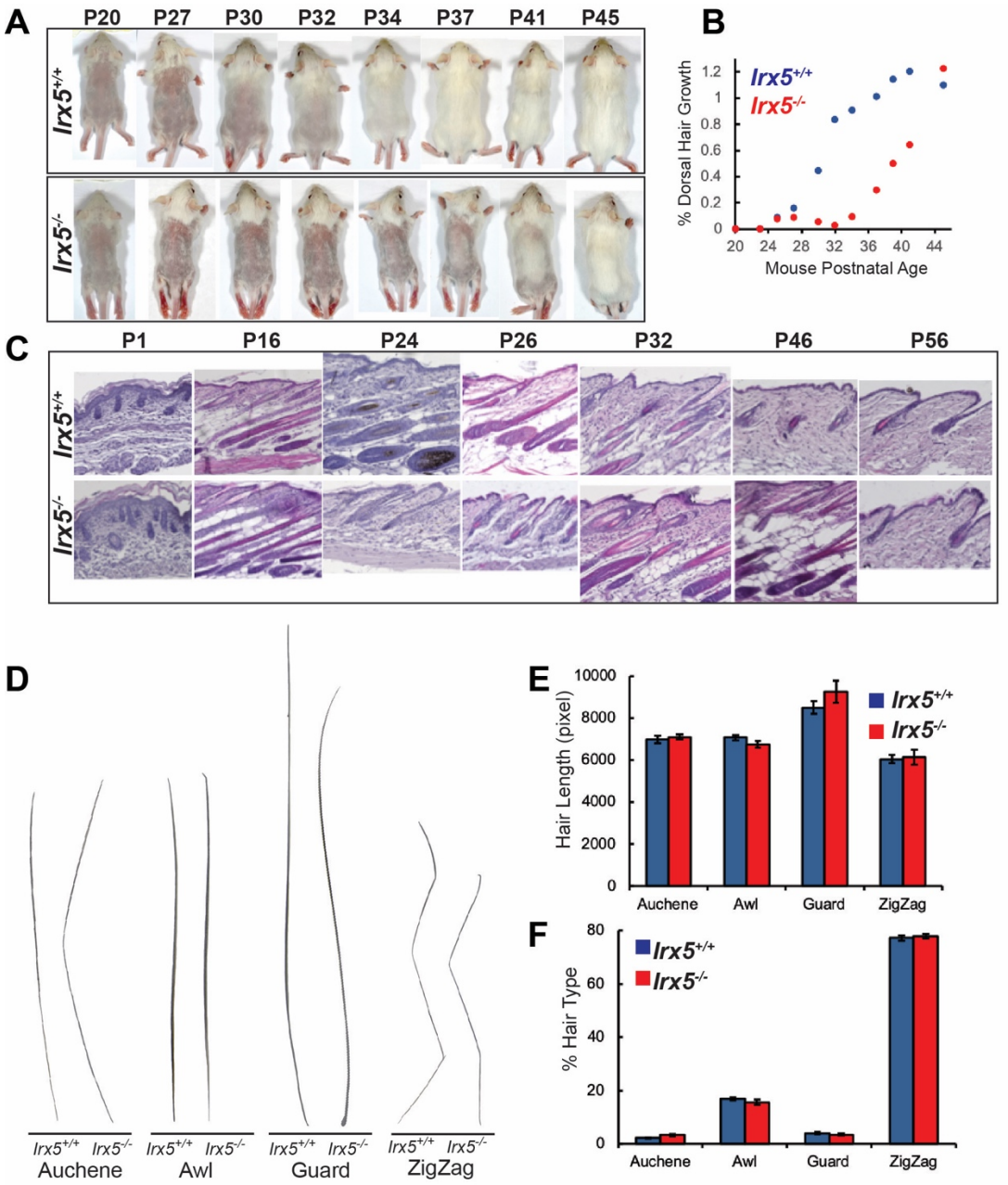

Figure 3.4: IRX5 promotes anagen initiation in mice.

A) Hair regrowth after shaving. Shown are representative *Irx5*$^{-/-}$ and *Irx5*$^{+/+}$ littermates. Back fur was shaved off at P20 and fur growth was documented until full recovery. B) Quantification of dorsal hair growth between 3 sets of littermates (n=6) per condition. C) Representative H&E histology of *Irx5*$^{-/-}$ and *Irx5*$^{+/+}$ dorsal epidermis at the indicated timepoints from the end of morphogenesis through the 1st hair cycle. D) Representative samples of hair fibers plucked from P20 *Irx5*$^{+/+}$ and Irx5$^{-/-}$ littermates. 100 hair fibers each from *Irx5*$^{+/+}$ (n=2) and *Irx5*$^{-/-}$ (n=2) littermates were E) measured to identify differences in hair length and F) counted to identify differences in the proportion of hair fiber types.

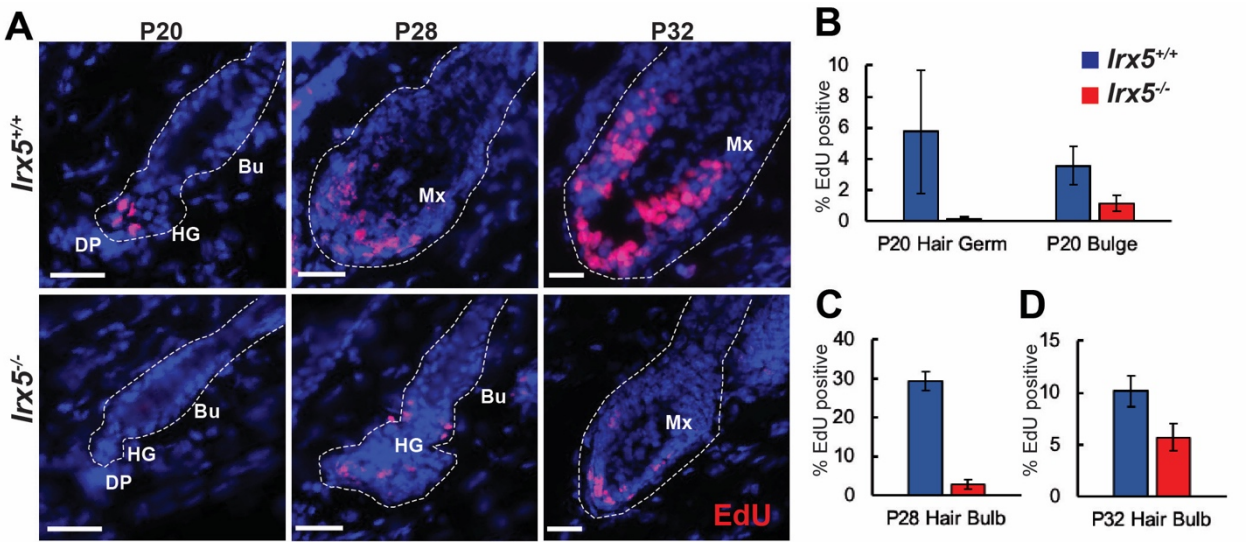

Figure 3.5: IRX5 promotes proliferation in hair germ and matrix cells.
A) Representative EdU staining in P20, P28, and P32 hair follicles from *Irx5*$^{-/-}$ and *Irx5*$^{+/+}$ littermates. B-D) Quantification of the percent of EdU-positive cells in the indicated locations *Irx5*$^{-/-}$ and *Irx5*$^{+/+}$ mice at P20 (B), P28 (C), and P32 (D).

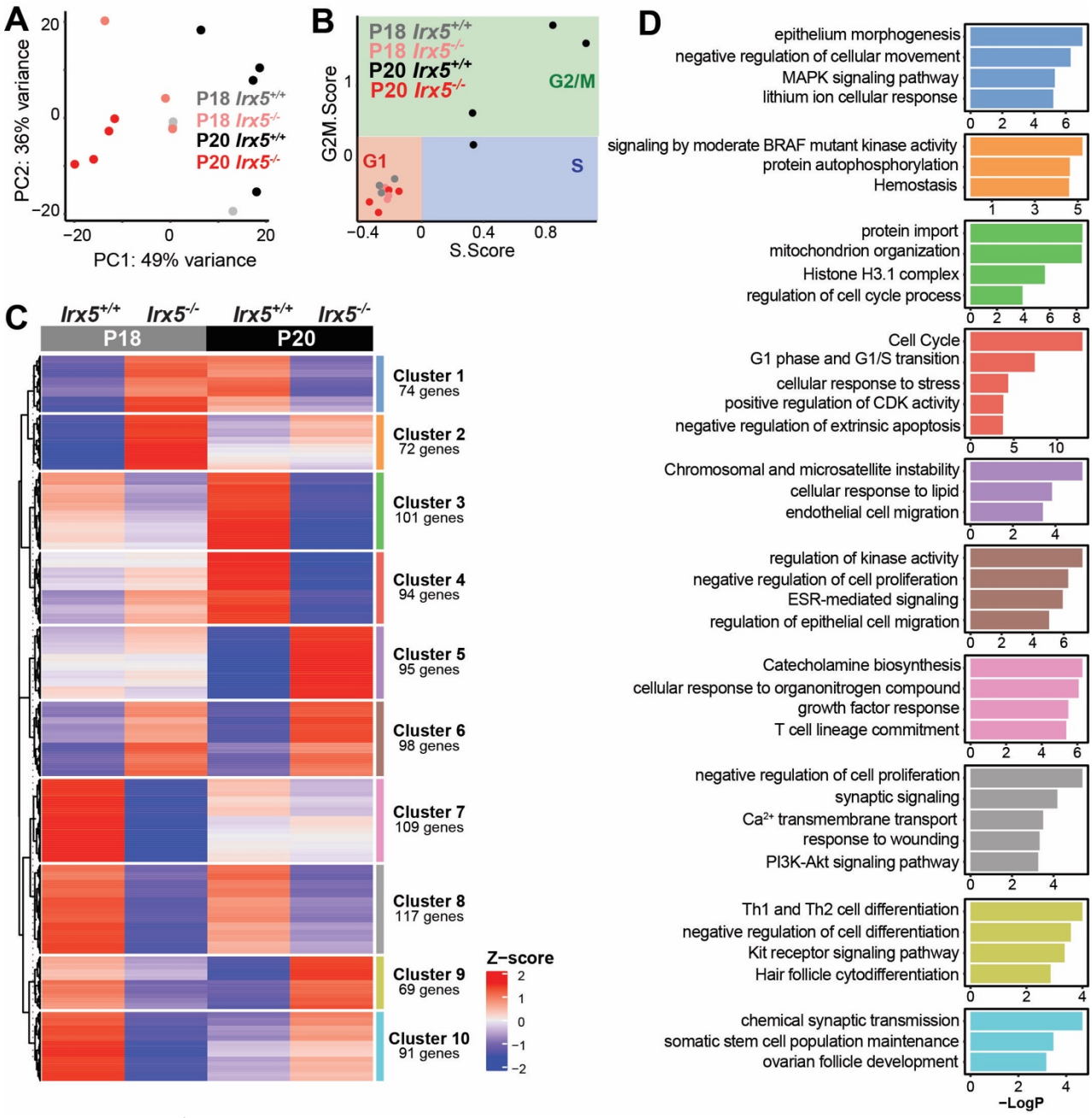

Figure 3.6: *Irx5*$^{-/-}$ display defective cell cycle

A) Principle component analysis of P18 *Irx5*$^{-/-}$ (n=3) and its *Irx5*$^{+/+}$ (n=3) littermates along with P20 *Irx5*$^{-/-}$ (n=4) and its *Irx5*$^{+/+}$ (n=4) littermates. B) Seurat cell cycle scoring was adapted to each replicate in bulk-RNAseq samples to identify the overall cell cycle stage of all HFSC isolated from each mice. C) Hierarchical clustering of P18 and P20 bulk RNA-seq samples identified 10 distinct gene clusters. D) Top gene ontology categories for each cluster.

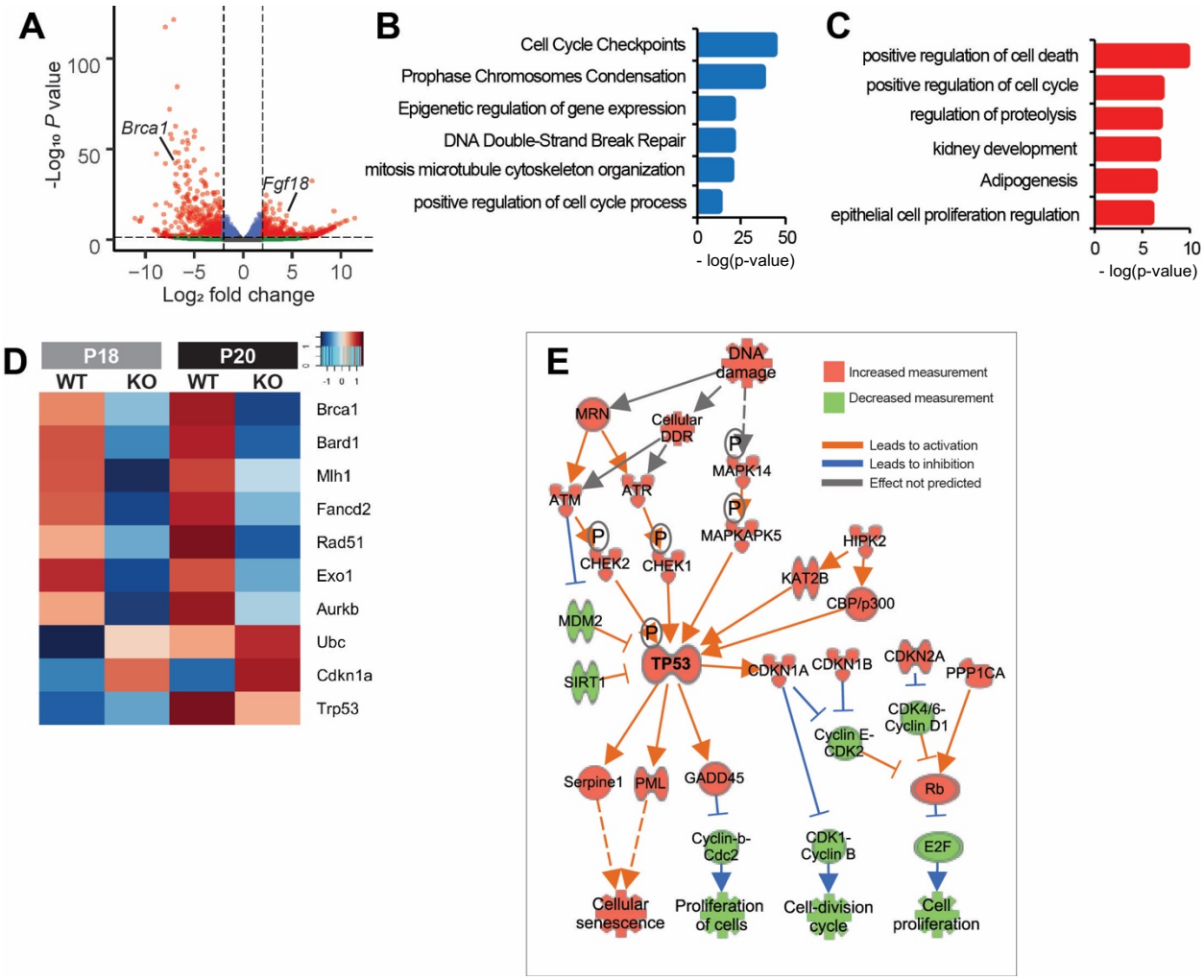

Figure 3.7: P20 *Irx5*$^{-/-}$ HFSC display defective cell cycle

A) Volcano plot of differentially expressed genes between P20 *Irx5*$^{-/-}$ HFSC and P20 *Irx5*$^{+/+}$ HFSC. Brca1 is downregulated and Fgf18 is upregulated in *Irx5*$^{-/-}$ HFSC. B) Gene ontology enrichment of downregulated genes. C) Gene ontology enrichment of upregulated genes. D) Heatmap of averaged expression of genes involved in DNA damage repair. E) QIAGEN Ingenuity Pathway Analysis predicted perturbed DNA damage in P20 *Irx5*$^{-/-}$ HFSC.

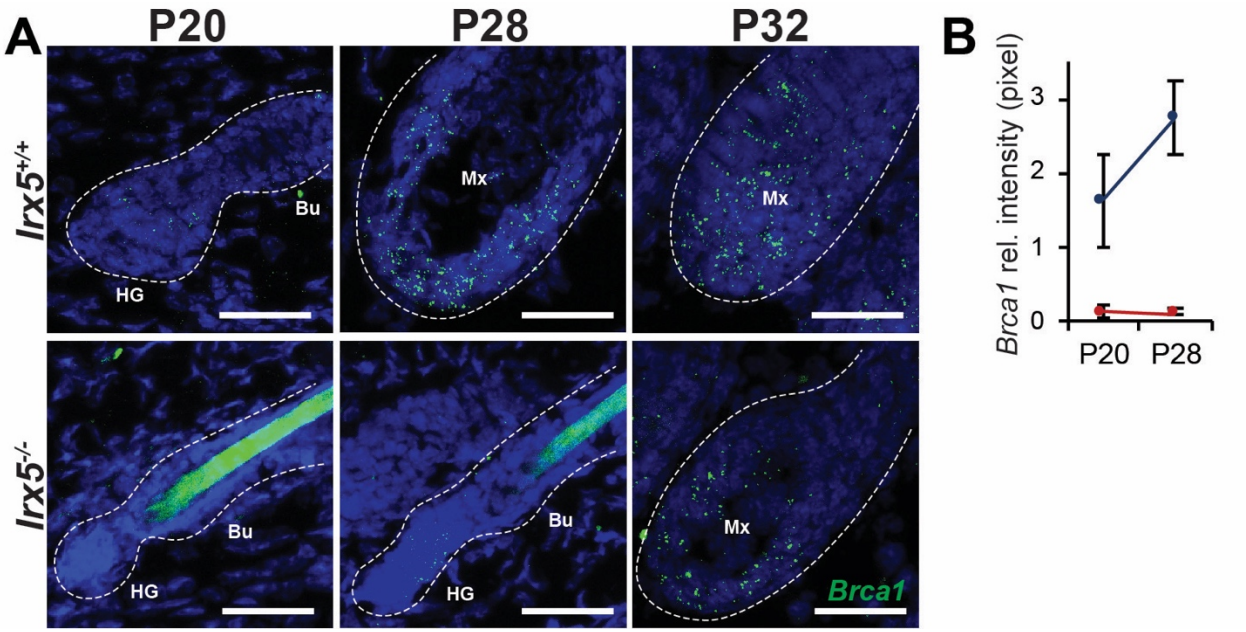

Figure 3.8: *Brca1* is downregulated P20 *Irx5*$^{-/-}$ HFSC

A) RNA FISH staining of *Brca1* in p20, p28, and p32 follicles from *Irx5*$^{-/-}$ and *Irx5*$^{+/+}$ mice. H) Quantification of *Brca1* signal intensity in p20 *Irx5*$^{-/-}$ (n=2), p20 *Irx5*$^{+/+}$ (n=2), p28 *Irx5*$^{-/-}$ (n=2), p28 *Irx5*$^{+/+}$ (n=2) hair follicles.

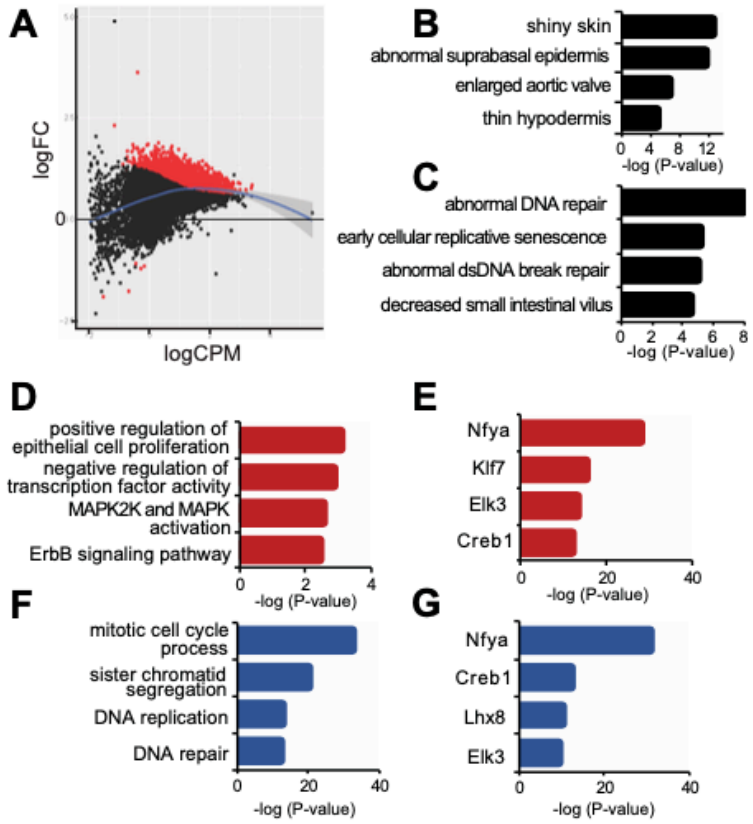

Figure 3.9: IRX5 maintains closed chromatin at DNA repair genes in hair follicle stem cells. A) ATAC-seq on *Irx5*$^{+/+}$ (n=2) and *Irx5*$^{-/-}$ (n=2) P20 HFSC identified differential open chromatin regions. The majority of differential chromatin regions represent accessible chromatin in *Irx5-/-* HFSC. B) Top mouse phenotype ontology categories associated with *Irx5*$^{+/+}$ HFSC open chromatin regions. C) Top mouse phenotype ontology categories associated with *Irx5*$^{-/-}$ HFSC open chromatin regions. D) Gene ontology of differential open chromatin regions associated with upregulated genes in P20 *Irx5*$^{-/-}$ HFSC. E) Enriched transcription factor binding motifs in differential open chromatin regions associated with upregulated genes in P20 *Irx5*$^{-/-}$ HFSC. F) Gene ontology of differential open chromatin associated with downregulated genes in P20 *Irx5*$^{-/-}$ HFSC. G) Enriched motif of differential open chromatin associated with downregulated genes in P20 *Irx5*$^{-/-}$ HFSC.

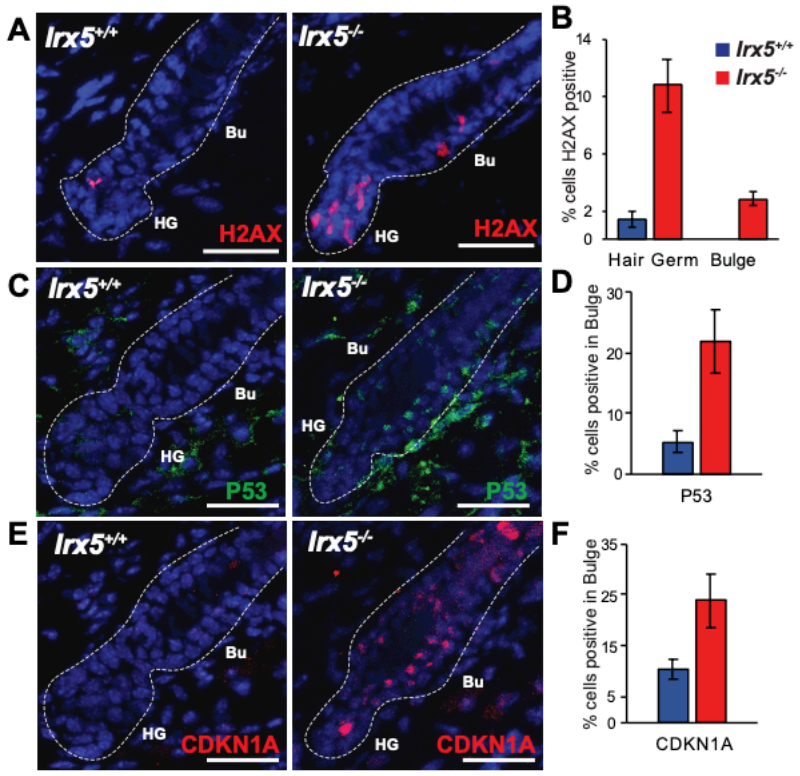

Figure 3.10: IRX5 is required for DNA damage repair and cell cycle progression in hair follicle stem cells.

A) Representative images of H2AX staining in the lower bulge p<0.0001 and hair germ p=0.02 of *Irx5*$^{-/-}$ and *Irx5*$^{+/+}$ littermates. B) Quantification of H2AX-positive *Irx5*$^{-/-}$ (n=20) and *Irx5*$^{+/+}$ (n=25) hair follicles. C) Representative images of P53 staining. D) Quantification of P53-positive bulge cells of *Irx5*$^{-/-}$ (n=15) and *Irx5*$^{+/+}$ (n=20) hair follicles. p=0.0078 E) Representative images of CDKN1A staining. F) Quantification of CDKN1A-positive bulge cells from *Irx5*$^{-/-}$ (n=3)and *Irx5*$^{+/+}$ mice. (n=4) p=0.04

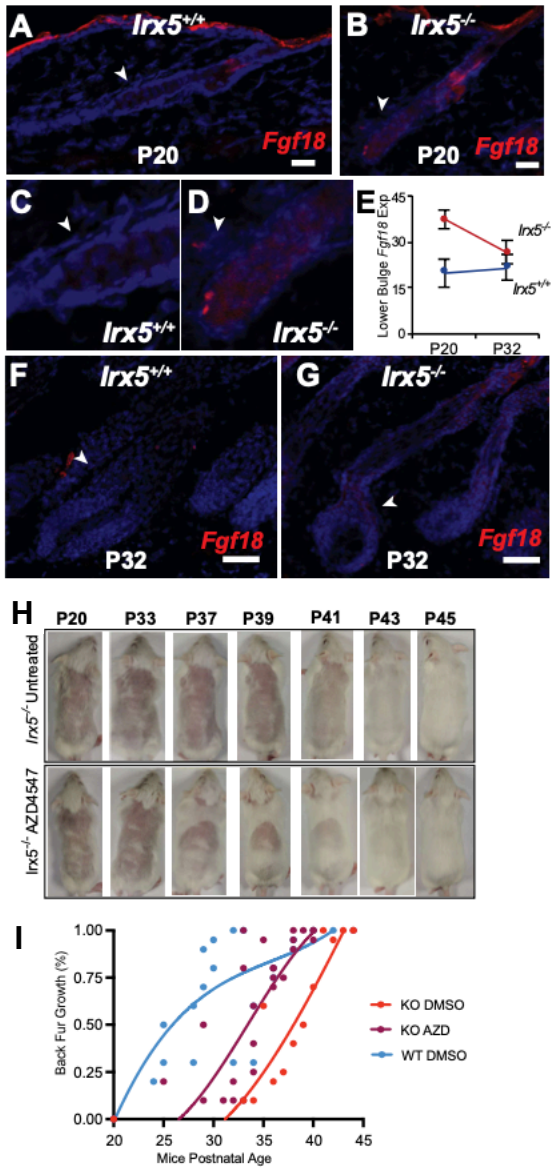

Figure 3.11: IRX5 suppresses the expression of Fgf18 in the hair follicle bulge during early anagen.

A-B) RNA in situ hybridization of Fgf18 in P20 hair follicles with arrows pointing to lower bulge. C-D) Higher magnification images of the lower bulge. E) Quantification of pixel intensity of lower bulge *Fgf18* signal in hair follicles from the indicated stages in *Irx5*$^{-/-}$ and *Irx5*$^{+/+}$mice. F-G) RNA in situ hybridization of *Fgf18* in P32 hair follicles with arrows pointing to lower bulge. H) Representative hair growth after shaving at P20 in *Irx5*$^{-/-}$ untreated and Irx5$^{-/-}$ mice treated with AZD4547. I) Quantification of hair growth through first Telogen and Anagen in untreated *Irx5*$^{+/+}$ (n=7), untreated *Irx5*$^{-/-}$ (n=9), and AZD4547-treated *Irx5*$^{-/-}$ mice (n=11).

Chapter 4: Methods

Mouse

Irx5$^{-/-}$ mice generation and genotyping has been described previously (139). Experiments were conducted on sex matched littermates. Mice was maintained on standard 12 hour light cycle with ad libitum food and water. All animal experiments were performed in accordance to University of California, Irvine Institutional Animal Care and Use Committee (Protocol No. AUP-19-012). To observe anagen hair follicle growth, the back fur was shaved at postnatal day 20 and mice were anesthetized and imaged every 3 days.

Hair follicle rescue experiments were conducted with AZD4547 (Selleckchem S2801) prepared in 4% DMSO, 5% PEG300, and 5% Tween80. Back fur was shaved at postnatal day 20 and 6mg/kg AZD4547 was administered every three days.

Tissue Isolation

P18 and P20 back skin was dissected and incubated in 0.25% trypsin (Invitrogen 1505-065) for 2hrs at 34C. The epidermal side was mechanically separated and resuspended in 2% FBS PBS. Debris was removed with 40uM and 70uM mesh filters. Whole epidermis samples were processed for bulk RNA-seq. For Hair follicle stem cells bulk RNAseq, cells were labeled with CD45f (eBioscience 12-0495), Ly-6A/E (eBioscience 45-5981-82), CD34 (eBioscience 50-0341-82), and DAPI. Ly-6A/E- CD34+ CD45f+ Hair follicle stem cells were isolated for bulk RNAseq and ATACseq.

Cell Culture: NHEK

Normal Human Epithelial Cells (NHEK) was obtained from donor neonatal foreskin and grown in Keratinocyte Serum Free Media supplemented with Epidermal Growth Factor and Bovine Pituitary Extract (Life Technologies). Individual Dharmacon on-TARGETplus siRNA [negative control (4390843), IRX2 (s45799, s45801), IRX3(s35710, s35712), IRX4(s55542, s27096), IRX5(s20056, s20054)] were validated and siRNA with at least 70% knockdown efficiency were pooled. 30nM pooled siRNA were transfected in semi-confluent monolayer with Lipofectamine RNAi Max (Life Technologies) in OptiMEM medium. 12 hours post transfection, 1.8mM Ca2+ was added into the growth medium to induce differentiation. RNA lysate was collected 72 hours after transfection.

Bulk RNA-sequencing

RNA quality was determined with Aglient Bioanalyzer with a cut off of RNA integrity Number > 8. Library preparation with Illumina TrueSeq library preparation kit and single end Illumina HiSeq 2500 sequencing was performed at University of California, Irvine High Throughput Genomics Facility. Read alignment was preformed using Tophat2 v2.0.10, and Cufflinks v2.2.0 was used for assembly, and Deseq2 was used to identify differentially expressed genes.

Quantitative real time PCR was used for validation of RNA-sequencing data. cDNA was prepared with iScript cDNA kit and RT-PCR was performed with Ssofast EvaGreen (Biorad) reagent in CX384 Real-Time PCR system (Biorad). GAPDH was used to normalize gene expression between samples.

ATACseq

Hair follicle stem cells (100,000 cells/replicate) were FACS sorted and lysed according to published protocols (140). Nuclei were incubated in 50uL of Tn5 transposition buffer for 30mins at 37C. DNA isolation was preformed with Qiagen MinElute Cleanup kit. Library preparation with Illumina TrueSeq library preparation kit and paired end Illumina HiSeq 2500 sequencing (80million reads per sample) was performed at University of California, Irvine High Throughput Genomics Facility. FASTQC was used to check read quality. Adapters were removed with cutadapt v2.9 (parameter: -a CTGTCTCTTATACACATCT -A CTGTCTCTTATACACATCT) and sequences were aligned and mapped to mm10 (UCSC) with Bowtie2 (141). Reads mapped to mitochondrial DNA was excluded. Following that, PCR duplicates were then removed based on the list of duplicate generated from Genrich (v0.6, available at github.com/jsh58/Genrich). Properly paired and mapped reads with mapping quality over 30 were kept for downstream analysis. To explore the feature of the uniquely mapped reads, deeptools (v3.4.2, parameter: -of bigwig --effectiveGenomeSize 2652783500 --normalizeUsing RPKM -e --ignoreDuplicates -bs 10) was used to convert aligned reads into a coverage track in BigWig format after read normalization based on RPKM. ChIPseeker (v1.24.0) was used to annotate the function of peaks.

RNA and protein detection

For immunofluorescence localization of protein, fresh tissue samples were harvested and embedded in OCT. 10uM sections were fixed in acetone at -20C for 10mins, fixed in 4% PFA for 10mins, permeabilized in 0.3% TritonX-100 for 10mins, and blocked in 0.5% BSA PBS for 1hr. Treated tissue was then incubated in primary antibody Krt14

(Abcam), Krt10 (Covance), p53bp1 (cell signaling), P21 (cell signaling), H2AX (cell signaling) overnight at 4C. Secondary antibodies were incubated at room temperature for 1hr. Images were captured with Keyence BZ-X700 or Nikon LSM780 confocal microscope.

For RNA Fluorescent *in situ* hybridization, fresh frozen 10uM thick OCT sections was processed and stained using RNAscope Multiplex Fluorescent Detection Kit v1 according to manufacturer's instructions. Processed samples were counterstained and preserved with ProLong Gold antifade reagent with DAPI. Images were captured on Nikon LSM780 confocal microscope.

Comparable images were post-processed in batches using the same maximum intensity projection and brightness setting for consistency. 2-6 biological replicates were analyzed for each marker.

Chapter 5: Conclusion

Adult stem cells have diverse methods for addressing DNA damage: In response to radiation, cycling intestinal stem cells undergo apoptosis while quiescent intestinal stem cells are radioresistant (103,104). In mammary stem cells, induced double stranded breaks (DSB) are efficiently repaired by p21 mediated Non-homologous end joining (NHEJ) (105,106). Melanocyte stem cells exposed to ionizing radiation triggers premature differentiation (107). HFSCs are resistant to DNA damage, in part due to elevated expression of DNA damage repair factors such as *Bcl-2* (108). BCL-2 suppresses DNA damage induced apoptosis and homologous recombination (HR), promoting the efficient but error prone non-homologous end joining (NHEJ) for DNA damage repair (109). However, in the absence of DNA damage repair factors such as BRCA1, HFSC display reduced proliferation, differentiation out of the stem cell niche, and apoptosis (113). Our work expands on this knowledge, identifying IRX5 as a novel upstream regulator of *Brca1* and other critical DNA damage repair genes.

Consistent with our findings, others have characterized the proliferative role of IRX5 in vascular smooth muscle cells and carcinomas (40,42,142). Here, we expand on these findings and provide preliminary evidence of the epigenetic mechanisms by which IRX5 influences the cell cycle. IRX factors mainly act as transcriptional repressors (143–147) though it can also act as transcriptional activators (148). Intriguingly, IRX activating or repressing function can be cell dependent or signaling dependent. In cerebellum formation, IRX4 is able to switch from activation to repression when induced by MAPK activation (148). In the transcription of a potassium channel, IRX5 is a activator in non-cardiac tissue and repressor in cardiomyocytes (144,149). The IRX protein comprises of

an IRO box, allowing it to form complexes with other transcription factors or epigenetic modifiers. This IRO box allows IRX5 to associate with m-BOP and recruit HDAC, promoting chromatin condensation and silencing transcription of nearby genes (144,150). These studies have suggested that IRX can regulate gene expression through complex formation with epigenetic modifiers.

In *Irx5*$^{-/-}$ HFSC, we identified unique open chromatin which were enriched in NF-Y motifs (Fig. 5.1). NF-Y is a transcription factor which binds to both repressed and activated chromatin marks, serving as both transcriptional activator or repressor (151). In response to DNA damage, NF-Y has been found to mediate transcriptional inhibition of cyclins during cell cycle arrest (152). At these NF-Y bound regions, cell cycle promoters are repressed through P53 dependent HDAC4 histone deacetylation (153). Our data suggests that IRX5 inhibits chromatin accessibility of repressive NF-Y binding sites near cell cycle progression genes. Here, we characterized open chromatin normally silenced in *Irx5*$^{+/+}$ HFSC with repressive signatures near cell cycle progression genes, suggesting IRX5 promotes proliferation through repressing the chromatin accessibility of these unique *Irx5*$^{-/-}$ HFSC regions.

From our transcriptome analysis, we honed in on BRCA1 as a downstream target of IRX5. At both mid and late telogen timepoints, *Brca1* was consistently downregulated in *Irx5*$^{-/-}$ HFSC, suggesting its differential expression to be due to the absence IRX5 independent of hair stage. Conditional knockout mouse model of *Brca1* in the epidermis displays a severe hair loss phenotype, with rapidly degenerating hair follicles due to increased apoptosis (113). While not as severe, *Irx5*$^{-/-}$ mice display similar key phenotypes as *Brca1*$^{-/-}$ mice such as increased DNA damage, decreased DNA damage

repair, and increased apoptosis. BRCA1 is a versatile factor involved in multiple DNA damage repair pathways, double stranded break processing, checkpoint regulation, and ubiquitination (128–130,154). Intriguingly, BRCA1 has been found to mediate heterochromatin maintenance, facilitating gene silencing (115). While further validation will need to be conducted, this could be an potential pathway by which IRX5 silences cell cycle repressive factors. BRCA1 is most notable for its role in hereditary breast and ovarian carcinomas. Recent work have linked IRX3 and IRX5 in ovarian follicle development (155), highlighting the importance IRX5 may play in these tissues. Previous reports have found that Fgf18 maintains HFSC quiescence and inhibits proliferation of hair germ (20). In response to DNA damage, Fgf18 induces cell cycle arrest and provides a longer period of time for DNA repair (138). These findings are consistent with the *Irx5*$^{-/-}$ HFSC phenotype, where increased DNA damage and concurrently observed with increased *Fgf18*. Partial rescue of the delayed anagen phenotype in *Irx5*$^{-/-}$ mice indicates that FGF18 is one of the downstream factors inhibited by IRX5.

One outstanding question left is why the intrafollicular epidermis remained unaffected by IRX5 deletion. During tissue homeostasis, epidermal stem cells proliferation is not coordinated as HFSC, where exogenous and internal signals activate HFSC in a cyclical fashion. Therefore, any cell cycle defect in *Irx5*$^{-/-}$ ESC does not ultimately affect IFE homeostasis. While we do observe DNA damage and similar resulting cellular responses in the ESC, the lack of an apparent epithelial phenotype suggests that there are other redundant factors promoting ESC proliferation. Perturbations such as

wounding or irradiation may elicit a more apparent epithelial phenotype as epithelial repair relies on massive ESC activation.

Thus, this study identifies IRX5 as a key mediator in DNA damage repair and HFSC activation. The findings from this study elucidates a small portion of the complex molecular mechanisms behind stem cell maintenance and activation. Further characterization of the proliferative role of IRX5 will provide key insights that can serve as the foundation for new targeted cancer therapies.

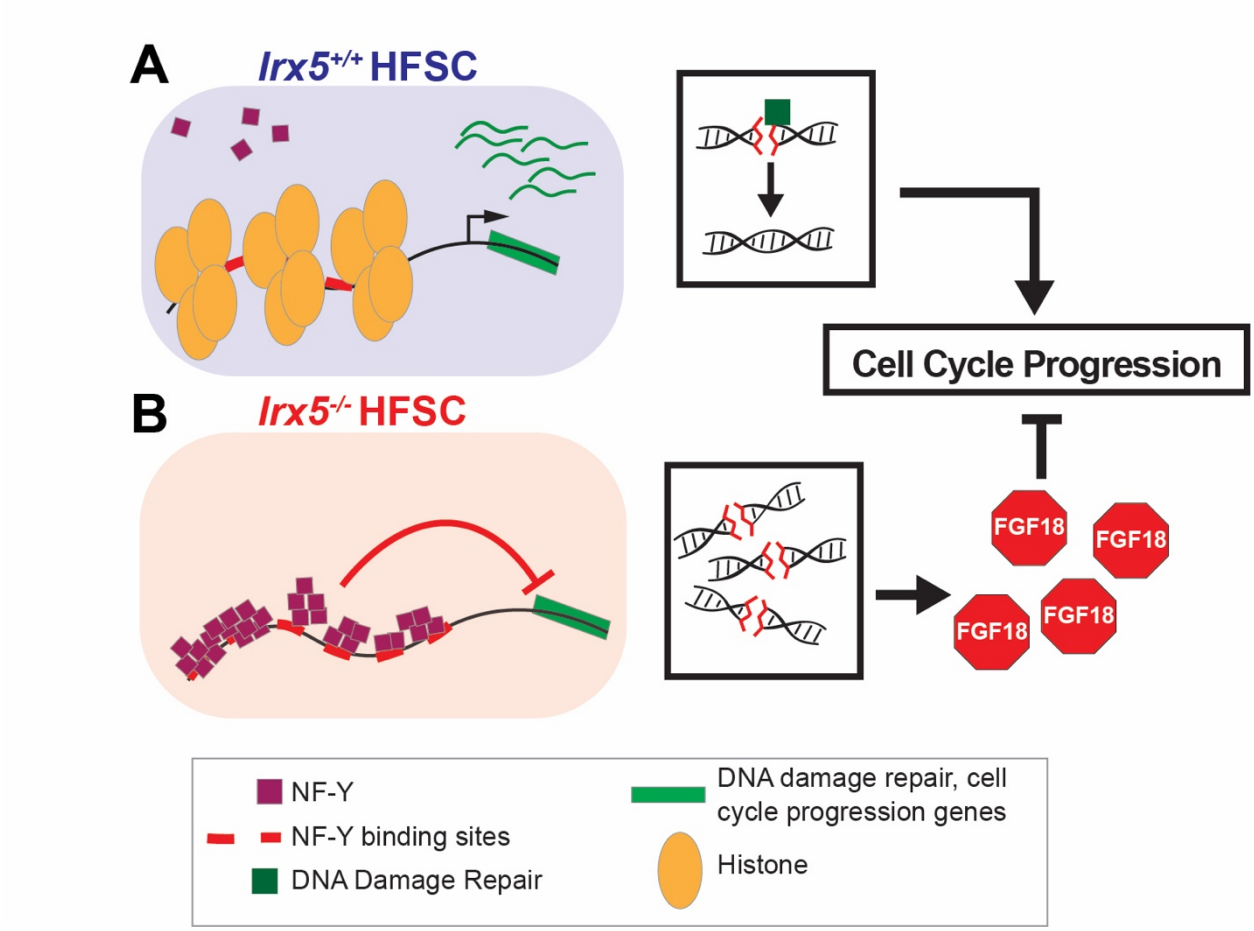

Figure 5.1: Model of IRX5 in DNA damage repair and proliferation.
Repressive NF-Y binding sites lie near genes which promote cell proliferation and DNA damage repair. A) In *Irx5*$^{+/+}$ HFSC, repressive NF-Y binding sites are closed, which allows for the transcription of genes involved in DNA damage repair and cell cycle progression. If any DNA damage occurs prior to replication, it is repaired. B) In contrast, the NF-Y binding sites in *Irx5*$^{-/-}$ HFSC is open, thus repressing the expression of DNA damage repair and cell cycle progression genes. Consequently, accumulation of DNA damage occurs which triggers cellular senescence.

References

1. Koster MI, Roop DR. Mechanisms Regulating Epithelial Stratification. Annu Rev Cell Dev Biol. 2007;23(1):93–113.

2. Fuchs E, Raghavan S. Getting under the skin of epidermal morphogenesis. Nat Rev Genet. 2002 Mar;3(3):199–209.

3. Wikramanayake TC, Stojadinovic O, Tomic-Canic M. Epidermal Differentiation in Barrier Maintenance and Wound Healing. Adv Wound Care. 2014 Jan 31;3(3):272–80.

4. Blanpain C, Fuchs E. Epidermal homeostasis: a balancing act of stem cells in the skin. Nat Rev Mol Cell Biol. 2009 Mar;10(3):207–17.

5. Candi E, Schmidt R, Melino G. The cornified envelope: a model of cell death in the skin. Nat Rev Mol Cell Biol. 2005 Apr;6(4):328–40.

6. Segre J. Complex redundancy to build a simple epidermal permeability barrier. Curr Opin Cell Biol. 2003 Dec;15(6):776–82.

7. Furuse M, Hata M, Furuse K, Yoshida Y, Haratake A, Sugitani Y, et al. Claudin-based tight junctions are crucial for the mammalian epidermal barrier a lesson from claudin-1–deficient mice. J Cell Biol. 2002 Mar 18;156(6):1099–111.

8. Feingold KR, Jiang YJ. The mechanisms by which lipids coordinately regulate the formation of the protein and lipid domains of the stratum corneum. Dermatoendocrinol. 2011 Apr 1;3(2):113–8.

9. Bikle DD. Vitamin D and the skin. J Bone Miner Metab. 2010 Jan 27;28(2):117–30.

10. Lopez-Pajares V, Qu K, Zhang J, Webster DE, Barajas BC, Siprashvili Z, et al. A LncRNA-MAF:MAFB Transcription Factor Network Regulates Epidermal Differentiation. Dev Cell. 2015 Mar 23;32(6):693–706.

11. Schneider MR, Schmidt-Ullrich R, Paus R. The Hair Follicle as a Dynamic Miniorgan. Curr Biol. 2009 Feb 10;19(3):R132–42.

12. Hoffman RM. The Pluripotency of Hair Follicle Stem Cells. Cell Cycle. 2006 Feb 1;5(3):232–3.

13. Schmidt-Ullrich R, Paus R. Molecular principles of hair follicle induction and morphogenesis. BioEssays. 2005;27(3):247–61.

14. Andl T, Reddy ST, Gaddapara T, Millar SE. WNT Signals Are Required for the Initiation of Hair Follicle Development. Dev Cell. 2002 May;2(5):643–53.

15. Rompolas P, Greco V. Stem cell dynamics in the hair follicle niche. Semin Cell Dev Biol. 2014 Jan 1;25(Supplement C):34–42.

16. Plikus MV, Mayer JA, de la Cruz D, Baker RE, Maini PK, Maxson R, et al. Cyclic dermal BMP signalling regulates stem cell activation during hair regeneration. Nature. 2008 Jan 17;451(7176):340–4.

17. Kobielak K, Stokes N, Cruz J de la, Polak L, Fuchs E. Loss of a quiescent niche but not follicle stem cells in the absence of bone morphogenetic protein signaling. Proc Natl Acad Sci. 2007 Jun 12;104(24):10063–8.

18. Horsley V, Aliprantis AO, Polak L, Glimcher LH, Fuchs E. NFATc1 Balances Quiescence and Proliferation of Skin Stem Cells. Cell. 2008 Jan 25;132(2):299–310.

19. Lee J, Hoi CSL, Lilja KC, White BS, Lee SE, Shalloway D, et al. Runx1 and p21 synergistically limit the extent of hair follicle stem cell quiescence in vivo. Proc Natl Acad Sci. 2013 Mar 19;110(12):4634–9.

20. Greco V, Chen T, Rendl M, Schober M, Pasolli HA, Stokes N, et al. A Two-Step Mechanism for Stem Cell Activation during Hair Regeneration. Cell Stem Cell. 2009 Feb 6;4(2):155–69.

21. Choi YS, Zhang Y, Xu M, Yang Y, Ito M, Peng T, et al. Distinct functions for Wnt/β-catenin in hair follicle stem cell proliferation and survival and interfollicular epidermal homeostasis. Cell Stem Cell. 2013 Dec 5;13(6):720–33.

22. Buecker C, Wysocka J. Enhancers as information integration hubs in development: lessons from genomics. Trends Genet. 2012 Jun 1;28(6):276–84.

23. Bulger M, Groudine M. Functional and Mechanistic Diversity of Distal Transcription Enhancers. Cell. 2011 Feb 4;144(3):327–39.

24. Blackwood EM, Kadonaga JT. Going the Distance: A Current View of Enhancer Action. Science. 1998 Jul 3;281(5373):60–3.

25. Rada-Iglesias A, Bajpai R, Swigut T, Brugmann SA, Flynn RA, Wysocka J. A unique chromatin signature uncovers early developmental enhancers in humans. Nature. 2011 Feb 10;470(7333):279–83.

26. Pott S, Lieb JD. What are super-enhancers? Nat Genet. 2015 Jan;47(1):8–12.

27. Whyte WA, Orlando DA, Hnisz D, Abraham BJ, Lin CY, Kagey MH, et al. Master Transcription Factors and Mediator Establish Super-Enhancers at Key Cell Identity Genes. Cell. 2013 Apr 11;153(2):307–19.

28. Hnisz D, Abraham BJ, Lee TI, Lau A, Saint-André V, Sigova AA, et al. Super-Enhancers in the Control of Cell Identity and Disease. Cell. 2013 Nov 7;155(4):934–47.

29. Adam RC, Yang H, Rockowitz S, Larsen SB, Nikolova M, Oristian DS, et al. Pioneer factors govern super-enhancer dynamics in stem cell plasticity and lineage choice. Nature. 2015 May 21;521(7552):366–70.

30. Saint-André V, Federation AJ, Lin CY, Abraham BJ, Reddy J, Lee TI, et al. Models of human core transcriptional regulatory circuitries. Genome Res. 2016 Mar 1;26(3):385–96.

31. Gómez-Skarmeta JL, Modolell J. araucan and caupolican provide a link between compartment subdivisions and patterning of sensory organs and veins in the Drosophila wing. Genes Dev. 1996 Nov 15;10(22):2935–45.

32. Calleja M, Herranz H, Estella C, Casal J, Lawrence P, Simpson P, et al. Generation of medial and lateral dorsal body domains by the pannier gene of Drosophila. Development. 2000 Sep 15;127(18):3971–80.

33. Gómez-Skarmeta JL, Glavic A, de la Calle-Mustienes E, Modolell J, Mayor R. Xiro, a Xenopus homolog of the Drosophila Iroquois complex genes, controls development at the neural plate. EMBO J. 1998 Jan 2;17(1):181–90.

34. Jessell TM. Neuronal specification in the spinal cord: inductive signals and transcriptional codes. Nat Rev Genet. 2000 Oct;1(1):20–9.

35. Peters T, Dildrop R, Ausmeier K, Rüther U. Organization of Mouse Iroquois Homeobox Genes in Two Clusters Suggests a Conserved Regulation and Function in Vertebrate Development. Genome Res. 2000 Oct;10(10):1453–62.

36. Bruneau BG, Bao Z-Z, Fatkin D, Xavier-Neto J, Georgakopoulos D, Maguire CT, et al. Cardiomyopathy in Irx4-Deficient Mice Is Preceded by Abnormal Ventricular Gene Expression. Mol Cell Biol. 2001 Mar 1;21(5):1730–6.

37. Cain CJ, Gaborit N, Lwin W, Barruet E, Ho S, Bonnard C, et al. Loss of Iroquois homeobox transcription factors 3 and 5 in osteoblasts disrupts cranial mineralization. Bone Rep. 2016 Dec;5:86–95.

38. Briscoe J, Pierani A, Jessell TM, Ericson J. A Homeodomain Protein Code Specifies Progenitor Cell Identity and Neuronal Fate in the Ventral Neural Tube. Cell. 2000 May 12;101(4):435–45.

39. Huang L, Song F, Sun H, Zhang L, Huang C. IRX5 promotes NF-κB signalling to increase proliferation, migration and invasion via OPN in tongue squamous cell carcinoma. J Cell Mol Med. 2018 Aug;22(8):3899–910.

40. Zhu L, Dai L, Yang N, Liu M, Ma S, Li C, et al. Transcription factorIRX5 promotes hepatocellular carcinoma proliferation and inhibits apoptosis by regulating the p53 signalling pathway. Cell Biochem Funct. 2020;38(5):621–9.

41. Myrthue A, Rademacher BLS, Pittsenbarger J, Kutyba-Brooks B, Gantner M, Qian DZ, et al. The Iroquois Homeobox Gene 5 Is Regulated by 1,25-Dihydroxyvitamin D3 in Human Prostate Cancer and Regulates Apoptosis and the Cell Cycle in LNCaP Prostate Cancer Cells. Clin Cancer Res. 2008 Jun 1;14(11):3562–70.

42. Liu D, Pattabiraman V, Bacanamwo M, Anderson LM. Iroquois homeobox transcription factor (Irx5) promotes G1/S-phase transition in vascular smooth muscle cells by CDK2-dependent activation. Am J Physiol - Cell Physiol. 2016 Aug 1;311(2):C179–89.

43. Schafer KA. The Cell Cycle: A Review. Vet Pathol. 1998 Nov 1;35(6):461–78.

44. Malumbres M, Barbacid M. Cell cycle, CDKs and cancer: a changing paradigm. Nat Rev Cancer. 2009 Mar;9(3):153–66.

45. Hochegger H, Takeda S, Hunt T. Cyclin-dependent kinases and cell-cycle transitions: does one fit all? Nat Rev Mol Cell Biol. 2008 Sep 24;9(11):910–6.

46. Sclafani RA, Holzen TM. Cell Cycle Regulation of DNA Replication. Annu Rev Genet. 2007;41(1):237–80.

47. Panier S, Boulton SJ. Double-strand break repair: 53BP1 comes into focus. Nat Rev Mol Cell Biol. 2014 Jan;15(1):7–18.

48. Scully R, Panday A, Elango R, Willis NA. DNA double-strand break repair-pathway choice in somatic mammalian cells. Nat Rev Mol Cell Biol. 2019 Nov;20(11):698–714.

49. Williams H, Flohr C. How epidemiology has challenged 3 prevailing concepts about atopic dermatitis. J Allergy Clin Immunol. 2006 Jul;118(1):209–13.

50. Cookson WOCM, Ubhi B, Lawrence R, Abecasis GR, Walley AJ, Cox HE, et al. Genetic linkage of childhood atopic dermatitis to psoriasis susceptibility loci. Nat Genet. 2001 Apr;27(4):372–3.

51. Palmer CNA, Irvine AD, Terron-Kwiatkowski A, Zhao Y, Liao H, Lee SP, et al. Common loss-of-function variants of the epidermal barrier protein filaggrin are a major predisposing factor for atopic dermatitis. Nat Genet. 2006 Apr;38(4):441–6.

52. Williams ML, Elias PM. Heterogeneity in autosomal recessive ichthyosis: Clinical and biochemical differentiation of lamellar ichthyosis and nonbullous congenital ichthyosiform erythroderma. Arch Dermatol. 1985 Apr 1;121(4):477–88.

53. Huber M, Rettler I, Bernasconi K, Frenk E, Lavrijsen SP, Ponec M, et al. Mutations of keratinocyte transglutaminase in lamellar ichthyosis. Science. 1995 Jan 27;267(5197):525–8.

54. Russell LJ, DiGiovanna JJ, Rogers GR, Steinert PM, Hashem N, Compton JG, et al. Mutations in the gene for transglutaminase 1 in autosomal recessive lamellar ichthyosis. Nat Genet. 1995 Mar;9(3):279–83.

55. De Castro SCP, Leung K, Savery D, Burren K, Rozen R, Copp AJ, et al. Neural tube defects induced by folate deficiency in mutant curly tail (Grhl3) embryos are associated with alteration in folate one-carbon metabolism but are unlikely to result from diminished methylation. Birt Defects Res A Clin Mol Teratol. 2010 Aug 1;88(8):612–8.

56. Ting SB, Caddy J, Hislop N, Wilanowski T, Auden A, Zhao L, et al. A Homolog of Drosophila grainy head Is Essential for Epidermal Integrity in Mice. Science. 2005 Apr 15;308(5720):411–3.

57. Yu Z, Lin KK, Bhandari A, Spencer JA, Xu X, Wang N, et al. The Grainyhead-like epithelial transactivator Get-1/Grhl3 regulates epidermal terminal differentiation and interacts functionally with LMO4. Dev Biol. 2006 Nov 1;299(1):122–36.

58. Caddy J, Wilanowski T, Darido C, Dworkin S, Ting SB, Zhao Q, et al. Epidermal Wound Repair Is Regulated by the Planar Cell Polarity Signaling Pathway. Dev Cell. 2010 Jul 20;19(1):138–47.

59. Yu Z, Bhandari A, Mannik J, Pham T, Xu X, Andersen B. Grainyhead-like factor Get1/Grhl3 regulates formation of the epidermal leading edge during eyelid closure. Dev Biol. 2008 Jul 1;319(1):56–67.

60. Hopkin AS, Gordon W, Klein RH, Espitia F, Daily K, Zeller M, et al. GRHL3/GET1 and Trithorax Group Members Collaborate to Activate the Epidermal Progenitor Differentiation Program. Bickmore WA, editor. PLoS Genet. 2012 Jul 19;8(7):e1002829.

61. Klein RH, Lin Z, Hopkin AS, Gordon W, Tsoi LC, Liang Y, et al. GRHL3 binding and enhancers rearrange as epidermal keratinocytes transition between functional states. PLOS Genet. 2017 Apr 26;13(4):e1006745.

62. Gordon WM, Zeller MD, Klein RH, Swindell WR, Ho H, Espetia F, et al. A GRHL3-regulated repair pathway suppresses immune-mediated epidermal hyperplasia. J Clin Invest. 2014 Dec 1;124(12):5205–18.

63. Rodríguez-Seguel E, Alarcón P, Gómez-Skarmeta JL. The Xenopus Irx genes are essential for neural patterning and define the border between prethalamus and thalamus through mutual antagonism with the anterior repressors Fezf and Arx. Dev Biol. 2009 May 15;329(2):258–68.

64. Claussnitzer M, Dankel SN, Kim K-H, Quon G, Meuleman W, Haugen C, et al. FTO Obesity Variant Circuitry and Adipocyte Browning in Humans. N Engl J Med. 2015 Sep 3;373(10):895–907.

65. Zhu L, van den Heuvel S, Helin K, Fattaey A, Ewen M, Livingston D, et al. Inhibition of cell proliferation by p107, a relative of the retinoblastoma protein. Genes Dev. 1993;7(7a):1111–25.

66. Feng L, Barnhart JR, Seeger RC, Wu L, Keshelava N, Huang S-H, et al. Cdc6 knockdown inhibits human neuroblastoma cell proliferation. Mol Cell Biochem. 2008 Apr 1;311(1–2):189–97.

67. Papetti M, Augenlicht LH. MYBL2, a link between proliferation and differentiation in maturing colon epithelial cells. J Cell Physiol. 2011 Mar 1;226(3):785–91.

68. Liu P, Kao TP, Huang H. CDK1 promotes cell proliferation and survival via phosphorylation and inhibition of FOXO1 transcription factor. Oncogene. 2008 Apr 14;27(34):4733–44.

69. Gopinathan L, Tan SLW, Padmakumar VC, Coppola V, Tessarollo L, Kaldis P. Loss of Cdk2 and Cyclin A2 Impairs Cell Proliferation and Tumorigenesis. Cancer Res. 2014 Jul 15;74(14):3870–9.

70. Zou L, Elledge SJ. Sensing DNA Damage Through ATRIP Recognition of RPA-ssDNA Complexes. Science. 2003 Jun 6;300(5625):1542–8.

71. Meyerson M, Harlow E. Identification of G1 kinase activity for cdk6, a novel cyclin D partner. Mol Cell Biol. 1994 Mar;14(3):2077–86.

72. Yan J, Jiang J, Lim CA, Wu Q, Ng H-H, Chin K-C. BLIMP1 regulates cell growth through repression of p53 transcription. Proc Natl Acad Sci. 2007 Feb 6;104(6):1841–6.

73. Chen C-F, Dou X-W, Liang Y-K, Lin H-Y, Bai J-W, Zhang X-X, et al. Notch3 overexpression causes arrest of cell cycle progression by inducing Cdh1 expression in human breast cancer cells. Cell Cycle. 2016 Feb 1;15(3):432–40.

74. Mantelli F, Argüeso P. Functions of ocular surface mucins in health and disease. Curr Opin Allergy Clin Immunol. 2008 Oct;8(5):477–83.

75. Hüffmeier U, Lascorz J, Becker T, Schürmeier-Horst F, Magener A, Ekici AB, et al. Characterisation of psoriasis susceptibility locus 6 (PSORS6) in patients with early

onset psoriasis and evidence for interaction with PSORS1. J Med Genet. 2009 Nov 1;46(11):736–44.

76. Caffery B, Joyce E, Heynen ML, Jones L, Ritter R, Gamache DA, et al. MUC16 expression in Sjogren's syndrome, KCS, and control subjects. Mol Vis. 2008 Dec 30;14:2547–55.

77. Felder M, Kapur A, Gonzalez-Bosquet J, Horibata S, Heintz J, Albrecht R, et al. MUC16 (CA125): tumor biomarker to cancer therapy, a work in progress. Mol Cancer. 2014 May 29;13(1):129.

78. Ornitz DM, Itoh N. The Fibroblast Growth Factor signaling pathway. Wiley Interdiscip Rev Dev Biol. 2015 May;4(3):215–66.

79. Schmidt MO, Garman KA, Lee YG, Zuo C, Beck PJ, Tan M, et al. The Role of Fibroblast Growth Factor-Binding Protein 1 in Skin Carcinogenesis and Inflammation. J Invest Dermatol. 2018 Jan 1;138(1):179–88.

80. Glotzer DJ, Zelzer E, Olsen BR. Impaired skin and hair follicle development in Runx2 deficient mice. Dev Biol. 2008 Mar 15;315(2):459–73.

81. Murayama K, Kimura T, Tarutani M, Tomooka M, Hayashi R, Okabe M, et al. Akt activation induces epidermal hyperplasia and proliferation of epidermal progenitors. Oncogene. 2007 Jul;26(33):4882–8.

82. Neufang G, Fürstenberger G, Heidt M, Marks F, Müller-Decker K. Abnormal differentiation of epidermis in transgenic mice constitutively expressing cyclooxygenase-2 in skin. Proc Natl Acad Sci U S A. 2001;98(13):7629–34.

83. Stuart T, Butler A, Hoffman P, Hafemeister C, Papalexi E, Mauck WM, et al. Comprehensive Integration of Single-Cell Data. Cell. 2019 Jun 13;177(7):1888-1902.e21.

84. Cabral A, Sayin A, de Winter S, Fischer DF, Pavel S, Backendorf C. SPRR4, a novel cornified envelope precursor: UV-dependent epidermal expression and selective incorporation into fragile envelopes. J Cell Sci. 2001 Nov 1;114(21):3837–43.

85. Jackson B, Tilli CMLJ, Hardman MJ, Avilion AA, MacLeod MC, Ashcroft GS, et al. Late Cornified Envelope Family in Differentiating Epithelia—Response to Calcium and Ultraviolet Irradiation. J Invest Dermatol. 2005 May 1;124(5):1062–70.

86. Stergiopoulos A, Elkouris M, Politis PK. Prospero-related homeobox 1 (Prox1) at the crossroads of diverse pathways during adult neural fate specification. Front Cell Neurosci. 2015;8:454.

87. Raveh E, Cohen S, Levanon D, Groner Y, Gat U. Runx3 is involved in hair shape determination. Dev Dyn. 2005;233(4):1478–87.

88. Hanakawa Y, Li H, Lin C, Stanley JR, Cotsarelis G. Desmogleins 1 and 3 in the Companion Layer Anchor Mouse Anagen Hair to the Follicle. J Invest Dermatol. 2004 Nov 1;123(5):817–22.

89. John S, Thiebach L, Frie C, Mokkapati S, Bechtel M, Nischt R, et al. Epidermal Transglutaminase (TGase 3) Is Required for Proper Hair Development, but Not the Formation of the Epidermal Barrier. PLOS ONE. 2012 Apr 4;7(4):e34252.

90. Rufini A, Tucci P, Celardo I, Melino G. Senescence and aging: the critical roles of p53. Oncogene. 2013 Oct;32(43):5129–43.

91. Barnes L, Dumas M, Juan M, Noblesse E, Tesniere A, Schnebert S, et al. γH2AX, an Accurate Marker That Analyzes UV Genotoxic Effects on Human Keratinocytes and on Human Skin. Photochem Photobiol. 2010;86(4):933–41.

92. Schultz LB, Chehab NH, Malikzay A, Halazonetis TD. P53 Binding Protein 1 (53bp1) Is an Early Participant in the Cellular Response to DNA Double-Strand Breaks. J Cell Biol. 2000 Dec 25;151(7):1381–90.

93. Lukas C, Savic V, Bekker-Jensen S, Doil C, Neumann B, Sølvhøj Pedersen R, et al. 53BP1 nuclear bodies form around DNA lesions generated by mitotic transmission of chromosomes under replication stress. Nat Cell Biol. 2011 Mar;13(3):243–53.

94. He G, Siddik ZH, Huang Z, Wang R, Koomen J, Kobayashi R, et al. Induction of p21 by p53 following DNA damage inhibits both Cdk4 and Cdk2 activities. Oncogene. 2005 Apr;24(18):2929–43.

95. de Pedro I, Galán-Vidal J, Freije A, de Diego E, Gandarillas A. p21CIP1 controls the squamous differentiation response to replication stress. Oncogene. 2021 Jan;40(1):152–62.

96. Molinuevo R, Freije A, Contreras L, Sanz JR, Gandarillas A. The DNA damage response links human squamous proliferation with differentiation. J Cell Biol [Internet]. 2020 Oct 1 [cited 2021 Jan 20];219(e202001063). Available from: https://doi.org/10.1083/jcb.202001063

97. Nguyen H, Merrill BJ, Polak L, Nikolova M, Rendl M, Shaver TM, et al. Tcf3 and Tcf4 are essential for long-term homeostasis of skin epithelia. Nat Genet. 2009 Oct;41(10):1068–75.

98. Petersson M, Brylka H, Kraus A, John S, Rappl G, Schettina P, et al. TCF/Lef1 activity controls establishment of diverse stem and progenitor cell compartments in mouse epidermis. EMBO J. 2011 Aug 3;30(15):3004–18.

99. Lay K, Kume T, Fuchs E. FOXC1 maintains the hair follicle stem cell niche and governs stem cell quiescence to preserve long-term tissue-regenerating potential. Proc Natl Acad Sci. 2016 Mar 15;113(11):E1506–15.

100. Wang L, Siegenthaler JA, Dowell RD, Yi R. Foxc1 reinforces quiescence in self-renewing hair follicle stem cells. Science. 2016 Feb 5;351(6273):613–7.

101. Rhee H, Polak L, Fuchs E. Lhx2 Maintains Stem Cell Character in Hair Follicles. Science. 2006 Jun 30;312(5782):1946–9.

102. Cheung TH, Rando TA. Molecular regulation of stem cell quiescence. Nat Rev Mol Cell Biol. 2013 Jun;14(6):329–40.

103. Roche KC, Gracz AD, Liu XF, Newton V, Akiyama H, Magness ST. SOX9 Maintains Reserve Stem Cells and Preserves Radioresistance in Mouse Small Intestine. Gastroenterology. 2015 Nov 1;149(6):1553-1563.e10.

104. Yousefi M, Li N, Nakauka-Ddamba A, Wang S, Davidow K, Schoenberger J, et al. Msi RNA-binding proteins control reserve intestinal stem cell quiescence. J Cell Biol. 2016 Oct 31;215(3):401–13.

105. Chang C-H, Zhang M, Rajapakshe K, Coarfa C, Edwards D, Huang S, et al. Mammary Stem Cells and Tumor-Initiating Cells Are More Resistant to Apoptosis and Exhibit Increased DNA Repair Activity in Response to DNA Damage. Stem Cell Rep. 2015 Sep 8;5(3):378–91.

106. Insinga A, Cicalese A, Faretta M, Gallo B, Albano L, Ronzoni S, et al. DNA damage in stem cells activates p21, inhibits p53, and induces symmetric self-renewing divisions. Proc Natl Acad Sci. 2013 Mar 5;110(10):3931–6.

107. Inomata K, Aoto T, Binh NT, Okamoto N, Tanimura S, Wakayama T, et al. Genotoxic Stress Abrogates Renewal of Melanocyte Stem Cells by Triggering Their Differentiation. Cell. 2009 Jun 12;137(6):1088–99.

108. Sotiropoulou PA, Candi A, Mascré G, De Clercq S, Youssef KK, Lapouge G, et al. Bcl-2 and accelerated DNA repair mediates resistance of hair follicle bulge stem cells to DNA-damage-induced cell death. Nat Cell Biol. 2010 Jun;12(6):572–82.

109. Wang Q, Gao F, May WS, Zhang Y, Flagg T, Deng X. Bcl2 Negatively Regulates DNA Double-Strand-Break Repair through a Nonhomologous End-Joining Pathway. Mol Cell. 2008 Feb 29;29(4):488–98.

110. Botchkarev VA, Komarova EA, Siebenhaar F, Botchkareva NV, Komarov PG, Maurer M, et al. p53 Is Essential for Chemotherapy-induced Hair Loss. Cancer Res. 2000 Sep 15;60(18):5002–6.

111. Kim JY, Ohn J, Yoon J-S, Kang BM, Park M, Kim S, et al. Priming mobilization of hair follicle stem cells triggers permanent loss of regeneration after alkylating chemotherapy. Nat Commun. 2019 Aug 27;10(1):3694.

112. Matsumura H, Mohri Y, Binh NT, Morinaga H, Fukuda M, Ito M, et al. Hair follicle aging is driven by transepidermal elimination of stem cells via COL17A1 proteolysis. Science [Internet]. 2016 Feb 5 [cited 2021 Sep 5]; Available from: https://www.science.org/doi/abs/10.1126/science.aad4395

113. Sotiropoulou PA, Karambelas AE, Debaugnies M, Candi A, Bouwman P, Moers V, et al. BRCA1 deficiency in skin epidermis leads to selective loss of hair follicle stem cells and their progeny. Genes Dev. 2013 Jan 1;27(1):39–51.

114. Wu J, Lu L-Y, Yu X. The role of BRCA1 in DNA damage response. Protein Cell. 2010 Feb 1;1(2):117–23.

115. Zhu Q, Pao GM, Huynh AM, Suh H, Tonnu N, Nederlof PM, et al. BRCA1 tumour suppression occurs via heterochromatin-mediated silencing. Nature. 2011 Sep;477(7363):179–84.

116. Keyes BE, Segal JP, Heller E, Lien W-H, Chang C-Y, Guo X, et al. Nfatc1 orchestrates aging in hair follicle stem cells. Proc Natl Acad Sci. 2013 Dec 17;110(51):E4950–9.

117. Sennett R, Wang Z, Rezza A, Grisanti L, Roitershtein N, Sicchio C, et al. An Integrated Transcriptome Atlas of Embryonic Hair Follicle Progenitors, Their Niche, and the Developing Skin. Dev Cell. 2015 Sep 14;34(5):577–91.

118. Hnisz D, Schuijers J, Lin CY, Weintraub AS, Abraham BJ, Lee TI, et al. Convergence of Developmental and Oncogenic Signaling Pathways at Transcriptional Super-Enhancers. Mol Cell. 2015 Apr 16;58(2):362–70.

119. Adam RC, Yang H, Rockowitz S, Larsen SB, Nikolova M, Oristian DS, et al. Pioneer factors govern super-enhancer dynamics in stem cell plasticity and lineage choice. Nature. 2015 May 21;521(7552):366–70.

120. Adam RC, Yang H, Ge Y, Lien W-H, Wang P, Zhao Y, et al. Temporal Layering of Signaling Effectors Drives Chromatin Remodeling during Hair Follicle Stem Cell Lineage Progression. Cell Stem Cell. 2018 Mar 1;22(3):398-413.e7.

121. Chen X, Whitney EM, Gao SY, Yang VW. Transcriptional Profiling of Krüppel-like Factor 4 Reveals a Function in Cell Cycle Regulation and Epithelial Differentiation. J Mol Biol. 2003 Feb 21;326(3):665–77.

122. Yoon HS, Chen X, Yang VW. Krüppel-like Factor 4 Mediates p53-dependent G1/S Cell Cycle Arrest in Response to DNA Damage *. J Biol Chem. 2003 Jan 24;278(4):2101–5.

123. Ma T, Tine BAV, Wei Y, Garrett MD, Nelson D, Adams PD, et al. Cell cycle–regulated phosphorylation of p220NPAT by cyclin E/Cdk2 in Cajal bodies promotes histone gene transcription. Genes Dev. 2000 Sep 15;14(18):2298–313.

124. Molden RC, Bhanu NV, LeRoy G, Arnaudo AM, Garcia BA. Multi-faceted quantitative proteomics analysis of histone H2B isoforms and their modifications. Epigenetics Chromatin. 2015 Apr 22;8(1):15.

125. Han M, Chang M, Kim U-J, Grunstein M. Histone H2B repression causes cell-cycle-specific arrest in yeast: Effects on chromosomal segregation, replication, and transcription. Cell. 1987 Feb 27;48(4):589–97.

126. Tagami H, Ray-Gallet D, Almouzni G, Nakatani Y. Histone H3.1 and H3.3 Complexes Mediate Nucleosome Assembly Pathways Dependent or Independent of DNA Synthesis. Cell. 2004 Jan 9;116(1):51–61.

127. Kaufman PD, Kobayashi R, Kessler N, Stillman B. The p150 and p60 subunits of chromatin assemblyfactor I: A molecular link between newly synthesized histories and DNA replication. Cell. 1995 Jun 30;81(7):1105–14.

128. Roy R, Chun J, Powell SN. BRCA1 and BRCA2: different roles in a common pathway of genome protection. Nat Rev Cancer. 2012 Jan;12(1):68–78.

129. Deng C-X. BRCA1: cell cycle checkpoint, genetic instability, DNA damage response and cancer evolution. Nucleic Acids Res. 2006;34(5):1416–26.

130. Zhao W, Steinfeld JB, Liang F, Chen X, Maranon DG, Jian Ma C, et al. BRCA1–BARD1 promotes RAD51-mediated homologous DNA pairing. Nature. 2017 Oct;550(7676):360–5.

131. McLean CY, Bristor D, Hiller M, Clarke SL, Schaar BT, Lowe CB, et al. GREAT improves functional interpretation of cis-regulatory regions. Nat Biotechnol. 2010 May;28(5):495–501.

132. Yun J, Chae H-D, Choi T-S, Kim E-H, Bang Y-J, Chung J, et al. Cdk2-dependent Phosphorylation of the NF-Y Transcription Factor and Its Involvement in the p53-p21 Signaling Pathway. J Biol Chem. 2003 Sep 19;278(38):36966–72.

133. Bonner WM, Redon CE, Dickey JS, Nakamura AJ, Sedelnikova OA, Solier S, et al. γH2AX and cancer. Nat Rev Cancer. 2008 Dec;8(12):957–67.

134. Feringa FM, Raaijmakers JA, Hadders MA, Vaarting C, Macurek L, Heitink L, et al. Persistent repair intermediates induce senescence. Nat Commun. 2018 Sep 25;9(1):3923.

135. Kimura-Ueki M, Oda Y, Oki J, Komi-Kuramochi A, Honda E, Asada M, et al. Hair Cycle Resting Phase Is Regulated by Cyclic Epithelial FGF18 Signaling. J Invest Dermatol. 2012 May 1;132(5):1338–45.

136. Leishman E, Howard JM, Garcia GE, Miao Q, Ku AT, Dekker JD, et al. Foxp1 maintains hair follicle stem cell quiescence through regulation of Fgf18. Development. 2013 Sep 15;140(18):3809–18.

137. Kawano M, Komi-Kuramochi A, Asada M, Suzuki M, Oki J, Jiang J, et al. Comprehensive Analysis of FGF and FGFR Expression in Skin: FGF18 Is Highly Expressed in Hair Follicles and Capable of Inducing Anagen from Telogen Stage Hair Follicles. J Invest Dermatol. 2005 May 1;124(5):877–85.

138. Kawano M, Umeda S, Yasuda T, Fujita M, Ishikawa A, Imamura T, et al. FGF18 signaling in the hair cycle resting phase determines radioresistance of hair follicles by arresting hair cycling. Adv Radiat Oncol. 2016 Jul 1;1(3):170–81.

139. Gaborit N, Sakuma R, Wylie JN, Kim K-H, Zhang S-S, Hui C-C, et al. Cooperative and antagonistic roles for Irx3 and Irx5 in cardiac morphogenesis and postnatal physiology. Development. 2012 Nov 1;139(21):4007–19.

140. Buenrostro JD, Wu B, Chang HY, Greenleaf WJ. ATAC-seq: A Method for Assaying Chromatin Accessibility Genome-Wide. Curr Protoc Mol Biol. 2015;109(1):21.29.1-21.29.9.

141. Langmead B, Salzberg SL. Fast gapped-read alignment with Bowtie 2. Nat Methods. 2012 Apr;9(4):357–9.

142. Sun X, Jiang X, Wu J, Ma R, Wu Y, Cao H, et al. IRX5 prompts genomic instability in colorectal cancer cells. J Cell Biochem. 2020;121(11):4680–9.

143. Bonnard C, Strobl AC, Shboul M, Lee H, Merriman B, Nelson SF, et al. Mutations in IRX5 impair craniofacial development and germ cell migration via SDF1. Nat Genet. 2012 Jun;44(6):709–13.

144. Costantini DL, Arruda EP, Agarwal P, Kim K-H, Zhu Y, Zhu W, et al. The Homeodomain Transcription Factor Irx5 Establishes the Mouse Cardiac Ventricular Repolarization Gradient. Cell. 2005 Oct 21;123(2):347–58.

145. Bjune J-I, Haugen C, Gudbrandsen O, Nordbø OP, Nielsen HJ, Våge V, et al. IRX5 regulates adipocyte amyloid precursor protein and mitochondrial respiration in obesity. Int J Obes. 2019 Nov;43(11):2151–62.

146. Gómez-Skarmeta J, de La Calle-Mustienes E, Modolell J. The Wnt-activated Xiro1 gene encodes a repressor that is essential for neural development and downregulates Bmp4. Dev Camb Engl. 2001 Feb;128(4):551–60.

147. Kudoh T, Dawid IB. Role of the iroquois3 homeobox gene in organizer formation. Proc Natl Acad Sci. 2001 Jul 3;98(14):7852–7.

148. Matsumoto K, Nishihara S, Kamimura M, Shiraishi T, Otoguro T, Uehara M, et al. The prepattern transcription factor Irx2, a target of the FGF8/MAP kinase cascade, is involved in cerebellum formation. Nat Neurosci. 2004 Jun;7(6):605–12.

149. He W, Jia Y, Takimoto K. Interaction between transcription factors Iroquois proteins 4 and 5 controls cardiac potassium channel Kv4.2 gene transcription. Cardiovasc Res. 2009 Jan 1;81(1):64–71.

150. Sims RJ, Weihe EK, Zhu L, O'Malley S, Harriss JV, Gottlieb PD. m-Bop, a Repressor Protein Essential for Cardiogenesis, Interacts with skNAC, a Heart- and Muscle-specific Transcription Factor *. J Biol Chem. 2002 Jul 19;277(29):26524–9.

151. Ceribelli M, Dolfini D, Merico D, Gatta R, Viganò AM, Pavesi G, et al. The Histone-Like NF-Y Is a Bifunctional Transcription Factor. Mol Cell Biol. 2008 Mar 15;28(6):2047–58.

152. Manni I, Mazzaro G, Gurtner A, Mantovani R, Haugwitz U, Krause K, et al. NF-Y Mediates the Transcriptional Inhibition of thecyclin B1, cyclin B2, and cdc25CPromoters upon Induced G2 Arrest. J Biol Chem. 2001 Feb 23;276(8):5570–6.

153. Basile V, Mantovani R, Imbriano C. DNA Damage Promotes Histone Deacetylase 4 Nuclear Localization and Repression of G2/M Promoters, via p53 C-terminal Lysines. J Biol Chem. 2006 Jan 27;281(4):2347–57.

154. Wu W, Koike A, Takeshita T, Ohta T. The ubiquitin E3 ligase activity of BRCA1 and its biological functions. Cell Div. 2008 Jan 7;3(1):1.

155. Fu A, Koth ML, Brown RM, Shaw SA, Wang L, Krentz KJ, et al. IRX3 and IRX5 collaborate during ovary development and follicle formation to establish responsive granulosa cells in the adult mouse†. Biol Reprod. 2020 Aug 21;103(3):620–9.